UMYU Scientifica, Vol. 3 NO. 4, December 2024, Pp 182 – 217
https://doi.org/10.56919/usci.2434.016
ISSN: 2955 – 1145 (print); 2955 – 1153 (online)
A periodical of the Faculty of Natural and Applied Sciences, UMYU, Katsina

ORIGINAL RESEARCH ARTICLE

Lithological and Structural Mapping of Basement Rock Units in the Ikara North-Central Basement Complex, Nigeria

Nana Fatima Abdulmalik[1] and Isiaka Ibrahim Ahmed[2]
[1]Centre for Energy Research and Training, Ahmadu Bello University, Zaria, Nigeria
[2]Department of Geology, Ahmadu Bello University, Zaria, Nigeria

ABSTRACT
The lithological and structural architecture to unravel the compositions and tectonic evolution of the Nigerian Basement Complex has not been fully documented by geoscientists. As such, this research aimed to investigate the lithological and structural characteristics of the Ikara North-Central Basement Complex. Detailed petrographic and field analysis reveals the prevalence of gneiss and granite lithologies characterized by significant structural features such as fractures, folds, and foliations. These findings offer new understandings of the tectonic evolution of the region. The study area mapped is the Ikara Sheet 103 Federal Survey Topographic Sheet to a scale of 1:100,000. The major lithological units underlying the study area are gneisses and granites. However, these major rock types have varieties, namely migmatitic gneiss, granite gneiss, migmatitic (augen) gneiss, porphyroblastic gneiss, medium to coarse-grained granites, and porphyritic granites. These rock types were intruded by quartzites, pegmatitic dykes, quartz, and aplite veins. Rock samples were observed and studied based on their mineralogical composition, color, and texture. The results of the petrographic analysis showed that the rocks are mainly composed of quartz, plagioclase feldspars, alkali feldspars, mica (biotite and muscovite), hornblende, garnet, and accessory minerals like zircon and magnetite. Geological structures were also observed during the field study, namely fractures (joints and fractures), foliations, lineations, veins, dykes, and various landforms. Photomicrographs from thin section analyses revealed micro-structures like myrmekites, micro-folds, and micro-fractures were also observed. Mineralization such as amethyst and cassiterite were hosted by quartz veins and pegmatites in porphyritic granites, respectively. A litho-structural map was produced, exhibiting the lithological units and regional structures cross-cutting the area of research.

ARTICLE HISTORY
Received August 12, 2024
Accepted October 15, 2024
Published October 29, 2024

KEYWORDS
Gneiss, Granites, Pegmatites, Fractures, Shear Zones

INTRODUCTION
Several orogenic series evolved during the collision of an active Pharusian continental margin of the Congo Craton and the passive continental margin of the West African Craton and gave rise to one of the major crustal complexes, which is the Nigerian Basement Complex (Burke and Dewey, 1972; Dada, 2006). This basement complex lies to the northwest of Congo Craton, east of West African Craton, and south of the Tuareg Shield (Burke and Dewey, 1972; Black *et al.*, 1979; LeBlanc, 1981; Caby *et al.*, 1981). The Nigerian Basement Complex makes up part of the Pan-African terrane that is considered to be the southern prolongation of the Central Hoggar by McCurry (1976). It is sometimes called the Neoproterozoic Trans-Saharan belt, which evolved as a result of the West African Craton colliding with the Congo Craton and the East Saharan block (Black *et al.*, 1994). According to Black and Lie´geois (1993), the East Saharan Block was probably a Craton up until 700 Ma. It was largely reactivated in a few areas, whereas the West African Craton was subducted beneath the Congo Craton (Grant *et al.*, 1972; Ball, 1980; Wright *et al.*, 1985). Caby (1989) and Boullier (1991) suggested that the Neoproterozoic Trans-Saharan Belt extends from North Africa to Brazil. However, sedimentary basins form, multiple collisions of island arcs, and continental fragments dating 750-500 Ma (Wright *et al.*, 1985; Ajibade and Wright, 1989) (Figure 1). It is a gamut between the Aïr Hoggar to the north (McCurry, 1976) and the Borborema Province to the south (Caby, 1989; Caby *et al.*, 1990).

The Nigerian Basement Complex and the Tuareg Shield differ from one another by the presence of higher grades of supracrustal in the Central Hoggar at the southern part of the Shield and the presence of extensive shear/mylonite zones in the Tuareg Shield, which divided the whole region into structural provinces (Ajibade *et al.*, 1987) (Figure 2). Although these types of structures occur in the Nigerian Basement, some N-S trending mylonite and fault

Correspondence: Abdulmalik, Nana Fatima. Centre for Energy Research and Training, Ahmadu Bello University, Zaria, Nigeria. ✉ nanafatima88@gmail.com
How to cite: Abdulmalik, N. F., & Ahmed, I. I. (2024). Lithological and Structural Mapping of Basement Rock Units in the Ikara North-Central Basement Complex, Nigeria. *UMYU Scientifica*, 3(4), 182–217. https://doi.org/10.56919/usci.2434.016

zones have also been recognized in the basement complex as well (Ajibade *et al.,* 1979; Hubbard, 1975). These Precambrian rocks are believed to have resulted from at least four key orogenic cycles of deformation, metamorphism, reactivation, and remobilization corresponding to the Liberian (2650 ± 150 Ma), the Eburnean (2000 ± 50 Ma), the Kibaran (1100 ± 200 Ma), and the Pan-African cycles (600 ± 150 Ma) (Grant, 1970; van Breemen *et al.,* 1977; Grant, 1978; Odeyemi, 1981; Rahaman *et al.*, 1983; Onyeagocha and Ekwueme, 1990; Obaje, 2009). Going by the International Geologic Time Scale in 2002, these ages correspond to Paleoarchean to Mesoproterozoic (3600 to 1600 Ma)) for Liberian and Eburnean; Mesoproterozoic to Neoproterozoic (1600 to 1000 Ma) for Kibaran; and Neoproterozoic to Early Paleozoic (1000 to 545 Ma) for Pan-African (Obiora, 2006). Each of the orogeny listed above has a unique structural imprint on the basement complex. As such, the Nigerian Basement Complex is associated with complex structures. However, the imprints of the first three cycles' have been largely overprinted by the latest and more prevalent Pan-African orogenic events. These have imposed structures with dominant trends of NNE-SSW, NE-SW, NNW-SSE, NW-SE, and N-S on the whole basement complex (Russ, 1957; McCurry, 1973; McCurry, 1976; Rahaman, 1988; Obaje, 2009).

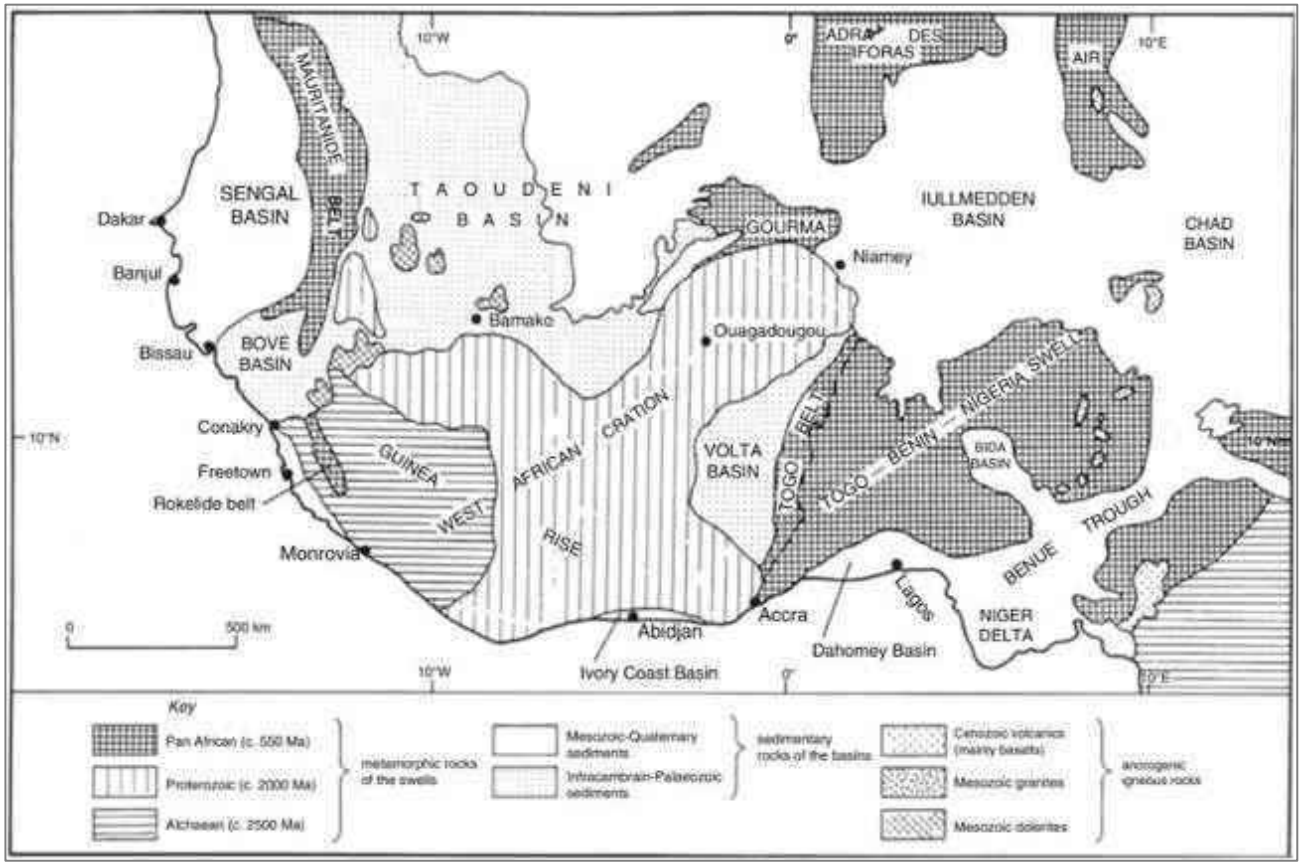

Figure 1: Geological map of Nigeria and West Africa (by extension) showing the various lithological units in the region (Wright *et al.*, 1985)

The Nigerian Basement Complex, a fragment of the Pan-African belt, is made of the older crusts of the Archean, Proterozoic, and Mesozoic ages (Grant, 1970; Grant *et al.*, 1972; Oversby, 1975; Dada, 1998). The Basement Complex was documented as an accumulation of juxtaposed terranes with migmatites, gneisses, Older Granites, and a sophisticated metasedimentary cover (Schist Belts) situated predominantly at the western part of the Basement, and a largely imperceptible crystalline terrane of mainly migmatites, gneisses, granite-diorite intrusions, and calc-silicate rocks the principally at the eastern part of the basement complex (Oyawoye, 1972; McCurry, 1976; Rahaman, 1976; Grant, 1978; Fitches *et al.*, 1985; Ajibade *et al.,* 1987; Onyeagocha and Ekwueme 1990; Dickin *et al.*, 1991; Ferre *et al.* 1995; Ferre´ *et al.*, 2002) (Figure 3). Ajibade *et al.* (1987) stated that the basement complex was separated into two main provinces: the western part was occupied mainly by the migmatites, gneisses, Schist Belts, and Older Granites, and the eastern part was occupied by migmatites, gneisses, and a large bulk of Pan-African granites intruded by Mesozoic Younger Granites. The basement complex was intruded by the Younger Granite suites, which are the alkaline and per-alkaline granites and volcanics of the Mesozoic age, emplaced in pre-existing lineaments, including a ring fracture (Ajibade *et al.*, 1987; Dada, 2006; Obaje, 2009). The Younger Granite intrusions are large extensive ring dykes that are irregular, relatively annular cylindrical, and sinuous with complex cross-cutting relationships and enclosed fragments of basement gneisses (Rahaman, 1988). However, about 50% of the basement complex is covered by sediments of Cretaceous to Recent age.

With all these being documented so far, delineating rock types and structural features to elucidate the tectonic framework of the north-central Basement Complex are yet to be documented in detail. Hence, this study aims to identify and discriminate the lithological and structural features of the Ikara Basement Complex. This will contribute to a better understanding of the region's tectonic evolution and mineralization potential."

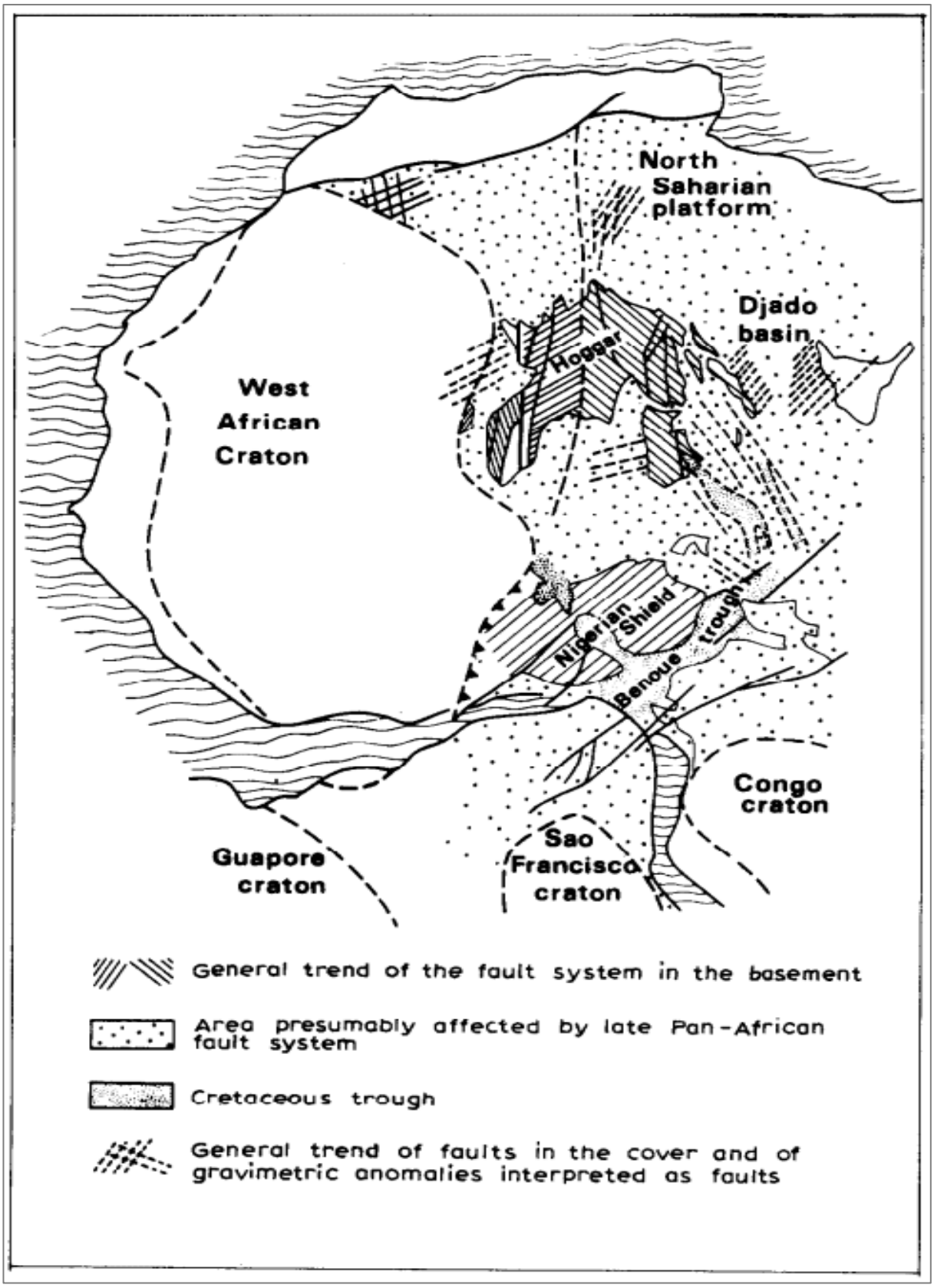

Figure 2: Geographical scope of the conjugate fault system in the Tuareg and Nigerian Shields and its potential extension into Brazil (adapted from Almeida and Black, 1967; in Ball, 1980).

MATERIALS AND METHODS

A systematic fieldwork was carried out using a topographic map at a scale of 1:100,000. The lithological units and structural features were identified and documented using the Geological compass and the Global Positioning System (GPS). Other instruments used during the fieldwork were a hand lens to view structures closely, a geologic (Brunton) compass to ascertain accurate direction trends, measure strike and dip values, a geological hammer to chip out representative rock samples, respectively, and measuring tape. Photographs of rock exposures, geological structures, landforms, and other important features were taken with the coordinates of the locations where these photographs were taken. Well-labeled representative rock samples were cut from exposures in the field, which were used for petrographic analysis in the thin section laboratory. This was carried out to identify mineralogical compositions of the rock samples and for microstructural analysis, using a geological microscope (in both plane-polarized light (PPL) and crossed polarized light (XPL)). Minerals and structures were identified at the micro-scale and other interpretations were outlined from further observations.

Study Area

The study area lies in the eastern province of the northcentral Nigerian Basement Complex. The geology is comprised of crystalline complex of migmatites, gneisses, and suites of intrusive syn-tectonic to late tectonic granites and granodiorites (McCurry, 1976; Ajibade *et al.*, 1987; Bruguier *et al.*, 1994; Ferre *et al.*, 1996; Dada, 1998, 2006; Abdulmalik, 2016; Abdulmalik *et al.*, 2018; Yusuf *et al.*, 2018; Fawwaz, 2019; Abdulmalik and Umaru, 2020). The area was affected by a series of deformational events such as the evolution of regional fractures, faults, joints, pegmatitic dykes, quartz and aplite veins, and shear zones characterized by cataclastic rocks, massive boulders, pulverized rocks, quartz breccias, discontinuous silicified quartzite ridges, sheared zones (Woakes *et al.*, 1987; Oluyide, 1988; Ajibade and Wright, 1989; Ferre *et al.*, 2002; Abdulmalik, 2016; Balarabe *et al.*, 2017). The Basement is enriched with several mineral resources and gemstones such as gold, cassiterite, beryl, aquamarine, amethyst, lithium, rare earth elements, etc., hosted in pegmatites (Garba, 2002, 2003; Abdulhamid, 2017; Ibrahim and Hayatu, 2021; Yusuf and Ibrahim, 2023).

Location of Study Area

The current area of study is part of the North-central Basement Complex at the north-western axis of Nigeria. The area is bounded by Latitudes 11° 00' 00" N to 11° 30' 00" N and Longitudes 08° 00' 00" E to 08° 30' 00" E. The study area falls within Ikara Sheet 103, at a scale of 1:100,000 of the topological map published by the Office of the Surveyor General of the Federation, Abuja, Nigeria (2008) (Figure 4). The total area coverage is approximately 3,032 square kilometers. Much of the area is within the Ikara, Tudun Wada, and Kiru Local Government Area Councils of Kaduna and Kano States, Nigeria. Makarfi, Soba, and Kubau Local Government Areas of Kaduna State and Kiru, Bebeji, and Tudun Wada Local Government Areas of Kano State bound the study area. The study area is accessible through the tarmac road that links many towns (e.g., Ikara, Anchau, Kargi, etc.) to the major dual Kaduna-Zaria-Kano highway, branching out at Tashar Yari, about 30km from Zaria. In addition, the study area is assessable from the southwest from Zaria Local Government Area, then into Gubuchi via Tashar Na Hawan Gubuchi of Makarfi LGA, Kaduna State via Kanawa single carriage road; from the southeast via a secondary road from Kargi-Chara-Tashar Bage towns of Ikara LGA, Kaduna State, and through Kubau LGA, Kaduna State; from the northeast from a partially tarred road from Tashar Dangara-Safara-Tudun Wada-Dankade of Tudun Wada LGA of Kano State, and via Tiga from Kiru/Bebeji LGA, Kano State; and the northwest via Kunkumi-Tarau or from Paki areas of Makarfi LGA, Kaduna State. The study area is also traversed by cattle tracks and footpaths through farmlands, several minor tarred and untarred roads linking several settlements.

Sampling method

Representative rock samples were randomly collected from lithological units exposed within the area of study for mineralogical and structural identification at the mesoscale and micro-scale. Samples of about average (13cm long and 10cm wide) dimensions were taken for analysis. However, getting fresh samples of some rocks was quite challenging, and thus, smaller samples were attained.

Data Collection

Data acquired during the field exercise for the research included coordinates of every station mapped; locations of where samples were taken; dimensions of the sizes of samples acquired; strike and dip values of lithological units; dimensional measurements of few outcrops; modal analyses; measurements of lineaments (fractures, joints, fold angle) used to produce Rose Diagrams; scale measurements and photographs of rock units and structural features of interest. All data were collated, analyzed, interpreted, and used to arrive at a meaningful conclusion for this research to be documented.

Laboratory Analyses

The laboratory analyses involved the usage of a petrographic (geological) microscope. This was utilized to identify the mineralogical compositions of the rocks and also identify microstructures that evolved during and after the rock formation process. Plane polarized light (PPL) and crossed polarized light (XPL) were used to describe the minerals in the rocks. A scale of 0.5mm and a magnification of (x40) were selected to identify occurring minerals and microstructural features for the thin-section analyses. Photographs of these thin-section slides viewed under the microscope were equally taken, adding to the documentation of this research.

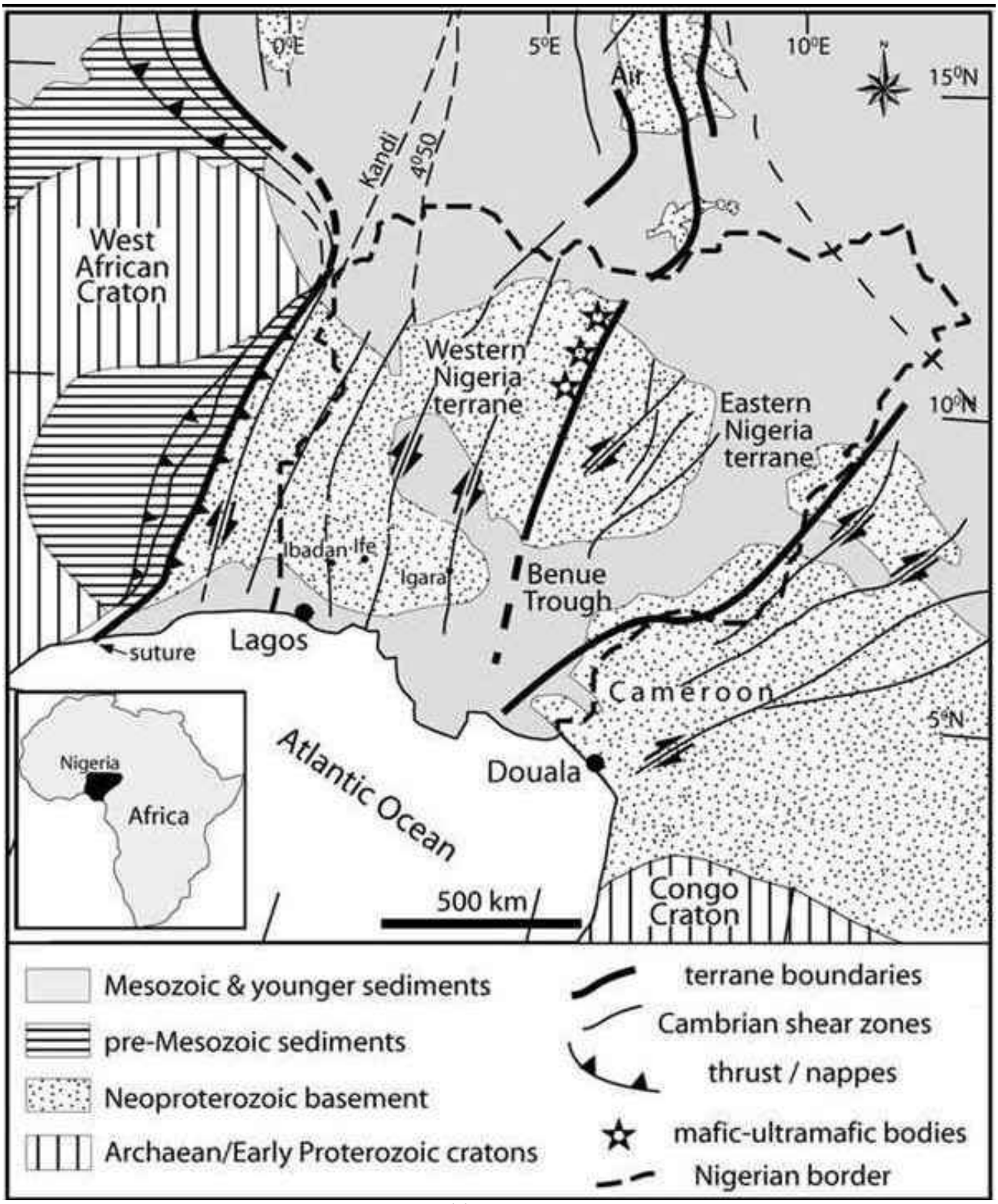

Figure 3: Geological map of the Neoproterozoic Trans-Saharan belt that resulted from the amalgamation of West African Craton, Congo Craton, and the East Saharan block. Terrane boundaries were recognized by Black *et al.* (1994). Inserted is a position of Nigeria in Africa.

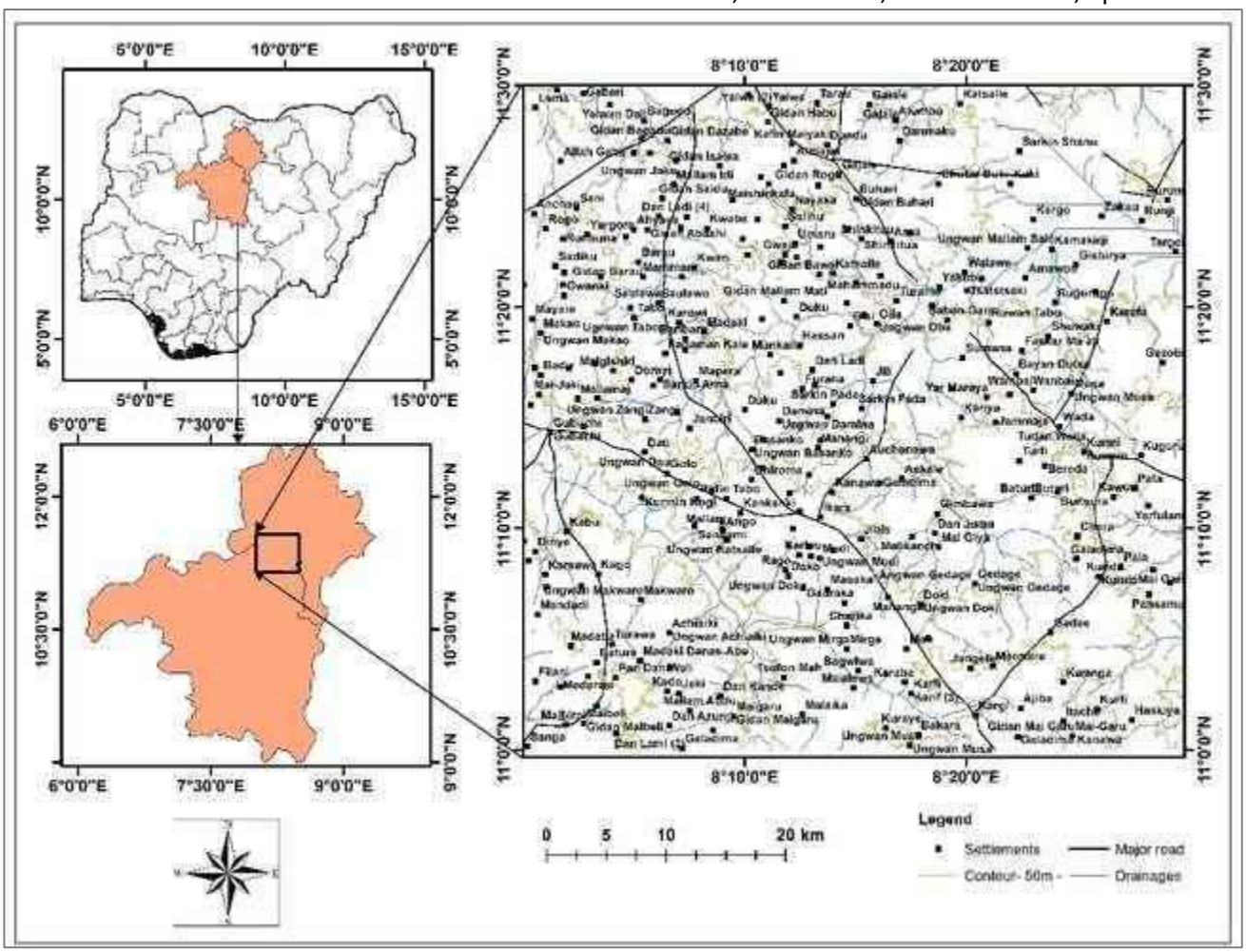

Figure 4: Map of the study area (right), which covers parts of Kaduna and Kano States (bottom left).

RESULTS AND DISCUSSIONS

LITHOLOGICAL DESCRIPTIONS

The study area predominantly comprises two major lithological units, namely gneiss and granite. The gneissic rocks have the following varieties: migmatitic-gneiss, migmatitic (augen) gneiss, Granite gneiss, and Porphyroblastic gneiss. Meanwhile, the granitic rocks are of two varieties namely medium to coarse-grained granite and porphyritic granite. Quartzites appeared mostly as discontinuous ridges that intruded the major rock units. They trended for several kilometers and are oriented NW-SE, NE-SW, and N-S. The migmatitic gneiss underlay part of the northwest, part of the northeast, part of the central region of the study area, and up north, southeast, and part of the eastern edge of the research area. Likewise, the migmatitic (augen) gneiss are found in the northeast, and the porphyroblastic gneisses are found in the west and southwestern regions of the research area. The medium to coarse-grained granite occupies a wide area in the northwest, and the porphyritic granites occupy an extensive area spanning from the southeast towards the south, east, northeast, and central areas of the study area. Pegmatites were also found to have intruded mostly the gneissic outcrops, and few intruded the granites in the form of veins and dykes.

Migmatitic Gneiss

This metamorphic rock unit was observed towards the northern parts of the study area (Figure 5). This lithology was at about 683m above mean sea level. The appearance of the lithology is gneissic, with the leucosome and mesosome (felsic and mafic minerals) alternatively layered in the form of foliation, otherwise termed gneissic banding or gneissosity. Migmatitic features such as ptygmatic foldings (Figure 6) were also observed on this type of gneiss. This lithology is flanked by medium-coarse-grained and porphyritic granites). It was observed that some parts of the migmatitic-gneiss identified towards the north-western part of the study area were sheared, having an N-S (354°) orientation. The lithology also trends in a NE-SW (056° to 070°) direction in other locations. They are rich in quartz, plagioclase alkali feldspars, mafic minerals like biotite, and accessory minerals, e.g. magnetite. This rock type underwent both brittle and ductile phases of deformations and, hence was highly fractured with a lot of joints, faults (sinistral strike-slip faults of veins and dykes with about 5 to 11cm displacement and dextral strike-slip faults with displacements between 2 to 9cm), xenoliths. This lithology appears mostly as whalebacks and domed-shaped.

Acquisition of fracture readings was used to plot a rose diagram and show an NW-SE direction as the dominant trend (Figure 7). Furthermore, petrographic analyses of these rocks showed mineral assemblages of plagioclase feldspar of about 34%, biotite of about 27%, quartz which constitutes about 20%, K-feldspar of about 14%, hornblende (3%) and some opaque minerals (2%).

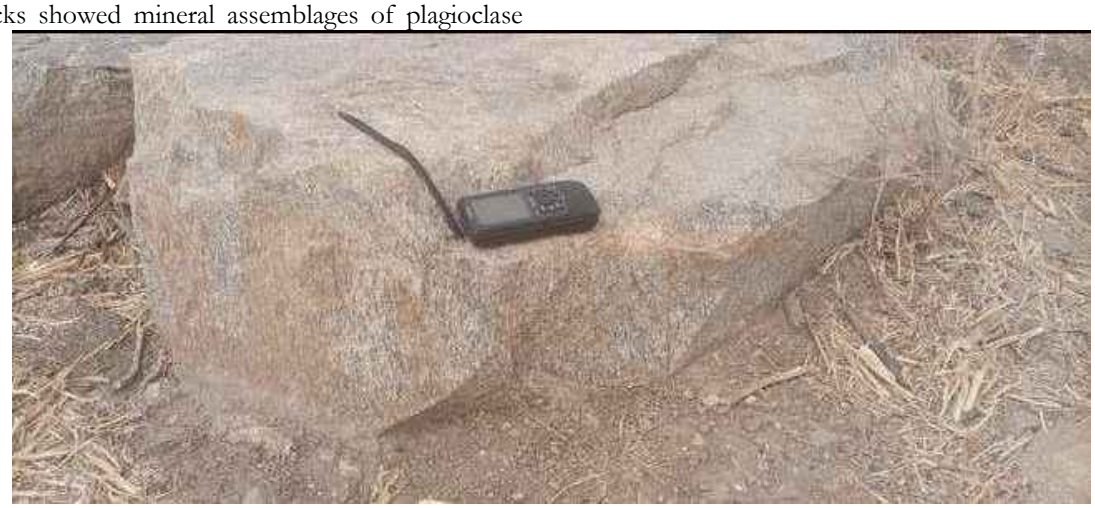

Figure 5: Migmatitic gneiss at Latitude 11° 29' 15" N and Longitude 08° 13' 01" E (Tarau).

Figure 6: Migmatitic gneiss located at Latitude 11° 26' 17" N and Longitude 08° 14' 09" E (Gajale).

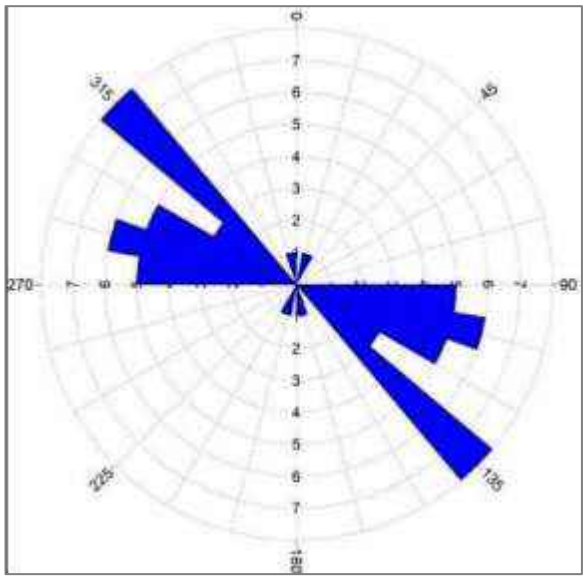

Figure 7: A rose diagram of strike readings of fractures on migmatitic gneiss, showing a dominant trend of NW-SE.

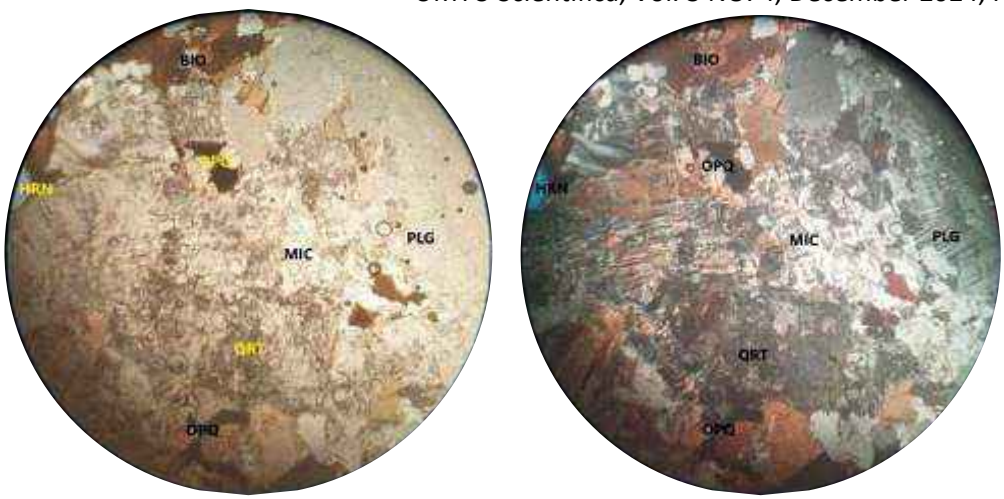

Figure 8: a: Photomicrograph of migmatitic-gneiss under PPL (Left). b: migmatitic-gneiss observed under XPL (Right). Biotite (BIO); Hornblende (HRN); Microcline (MIC); Plagioclase (PLG); Quartz (QRT). Magnification: x40; Scale: 0.5mm.

Migmatitic (Augen) Gneiss

These metamorphic rocks exhibited bandings of felsic and mafic minerals and migmatitic foliations, which were folded symmetrically at some parts of the outcrops due to differential stress (maximum stress) acting horizontally. There were some identified ptygmatic folding in some outcrops which are evidence of closeness to melting. It also has some large, porphyroblastic textures and sigmoidal minerals shaped in the form of an eye, hence named migmatite augen gneiss. These exposures have chilled intrusions with fine-grained texture, digested portions of younger rocks observed within the main lithology (Lith per Lith), and contact between them and medium to coarse-grained granite was observed. In some areas, like in the Kunkumi axis, some exposures of this lithology are sheared and trend in an N-S direction and have low landforms that appear to have evolved along a fault-shear zone (Figure 9). In addition, several lateralized quartzite ridges were observed at various locations trending NE-SW. Several cross-cutting joints, veins (measuring about 0.6cm to 3cm wide), pegmatite dykes (measuring about 10cm to 34.9cm wide), and pegmatitic veins (measuring about less than 1cm to 4.5cm wide), displacement of pegmatitic dykes were observed. Sinistral faults with displacements (4cm to 15cm) trending NW-SE and very few dextral faults were also seen with displacements (3cm to 9cm) trending NE-SW. Folding of veins and dykes, kinking of both foliated bands, and very narrow veins are exhibited by this rock type. In addition, several discontinuous quartzite ridges were observed cutting across this lithology, trending NE-SW, NW-SE, and N-S. A rose plot (Figure 10) shows a dominant trend of fractures to be NW-SE.

Photomicrograph analysis (Figure 11) was carried out, and it was observed that plagioclase was about 35%, biotite (26%), quartz (21%), K-feldspar (13%), hornblende (2%), and opaque minerals (3%) were identified. A few augen megacrysts were identified to be mostly quartz and plagioclase. Some biotite minerals were quite elongated, brecciated, and micro-folded at a few points around some quartz and plagioclase mineral grains. Several intragranular fractures were observed and filled with quartz. Some quartz minerals are chemically altered. Micro-foliations exhibited by platy elongated biotite minerals, and intergranular joints were observed in the slide.

Figure 9: Migmatitic (augen) gneiss; Latitude 11° 22' 57" N and Longitude 08° 02' 52" E (Gangarida).

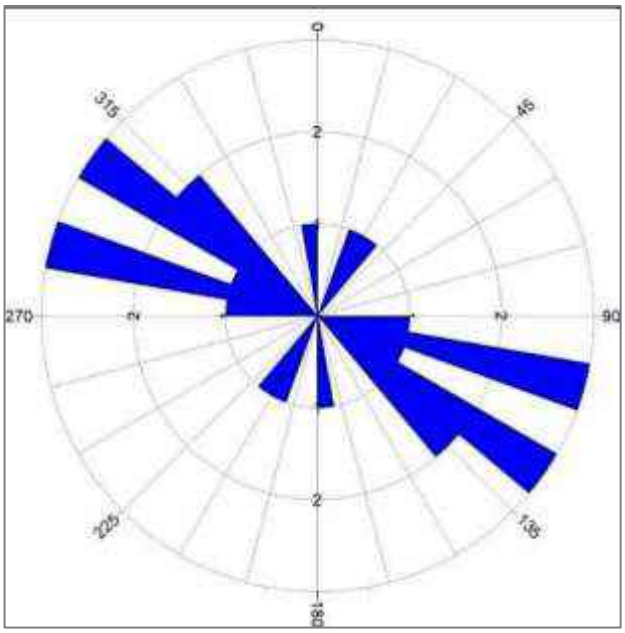

Figure 10: A rose plot showing NW-SE as the dominant trend of fractures on migmatitic (augen) gneiss.

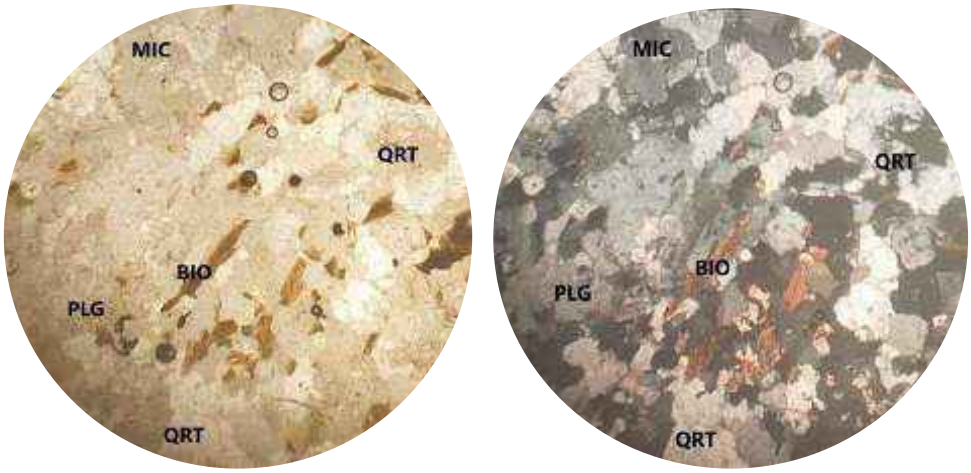

Figure 11: Photomicrograph of migmatitic (augen) gneiss in PPL (Left) and Plate XII: migmatitic (augen) gneiss under XPL (Right). Biotite (BIO); Microcline (MIC); Plagioclase (PLG); Quartz (QRT). Magnification: x40; Scale: 0.5mm.

Granite-Gneiss

These fine-grained textured exposures were in the form of boulders, low to moderately high domes, and whale-backs along and away from river channels (Figure 12). They are highly weathered on the surface with brownish, pale white to grey colorations. They are in contact with the medium to coarse-grained biotite granite and migmatite-gneiss lithologies. These evolved after the augen gneisses, predominantly made of plagioclase feldspar, quartz, biotite, and less alkali feldspar with grain sizes less than 1mm. Fresh samples show gneissic banding of alternating light and dark-colored minerals. They exhibit a series of cross-cutting joints of varying widths, some filled with quartz, aplite, or calcite, and are turned into veins with varying lengths ranging between 1.3cm to 5cm. Also observed were cross-cutting veins (diadysites), pegmatitic veins (18.1-21.2m in length and width values of 1-2cm), and dykes extending more than 47m in length and width values of 20-35cm. Some of the veins were folded/kinked, others were sinistrally (NW-SE fault line) and dextrally (NE-SW fault line) displaced (about 3cm to 15cm displacement), and xenoliths of younger rocks were observed on some of the outcrops. They strike at angles between 035º-070º NE and have dip values between 20º-58º (SE). Figure 13 is a rose diagram showing the directions of fractures within this lithology encountered in the field but shows the dominant trend of most of the fractures to be towards NW-SE. Photomicrograph of granite-gneiss (Figure 14) shows the dominance of plagioclase (30%), quartz (25%), biotite (26%), K-feldspar (15%), muscovite (2%), and opaque (2%). Some of the minerals were fractured and filled with possibly quartz. The textures of the rock are somewhat granitic, but micro-foliations were also observed.

Figure 12: Granite-gneiss at Ungwan Gangarda; Latitude 11° 23' 50"N and Longitude 08° 05' 58"E.

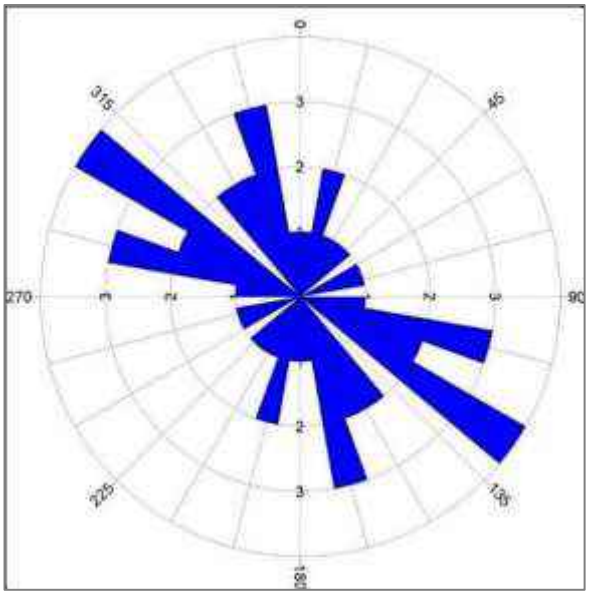

Figure 13: A rose plot indicating a NW-SE trend exhibited by most fractures on granite-gneiss.

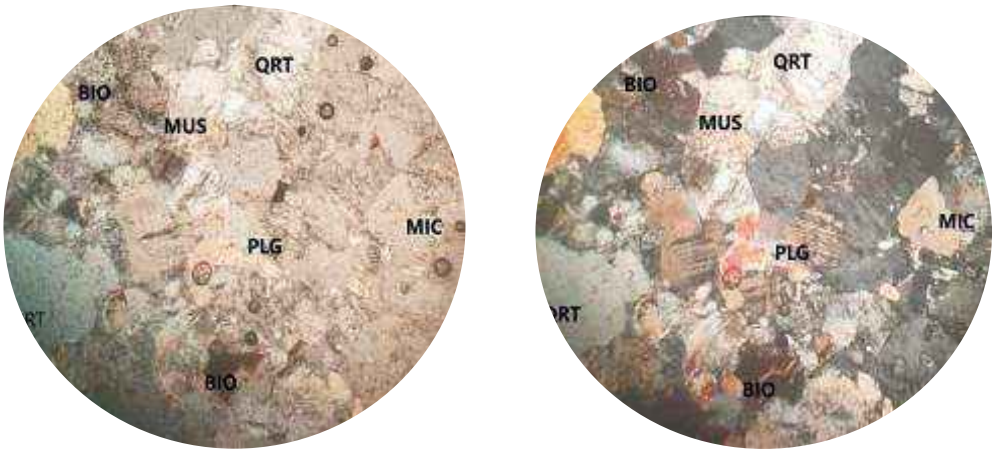

Figure 14: Photomicrograph of Granite-Gneiss in PPL (Left). Plate XV: Granite-Gneiss observed under XPL (Right). Biotite (BIO); Microcline (MIC); Muscovite (MUS); Plagioclase (PLG); Quartz (QRT). Magnification: x40; Scale: 0.5mm.

Porphyroblastic Gneiss

Porphyroblastic gneisses are gneisses observed to have granoblastic or metacrysts grains in the mix of fine to medium grain matrix (Figure 15). These exposures are prominent at the southwestern part of the study area which is an area densely covered by trees. They are in close contact with migmatite (augen) gneiss and, as such, could be easily mixed up because of the presence of large mineral grains (porphyroblasts) of orthoclase feldspars of

about 1cm to 1.5cm wide that lie in the fine matrix. It has several pegmatitic dykes ranging from 20cm to 34cm, and very few joints and veins between 1 to 3cm wide were seen. They occur as pockets of boulders in some areas and as whalebacks or low-laying domes in other areas. The rock is composed of alkali feldspar (40%), which are pinkish and forms the metacrysts, biotite (30%), quartz (25%), and plagioclase feldspars (5%). There were also systematic foldings identified in some of the exposures. The regions where these boulders occur are suggested to be possible shear zones because the porphyroblastic grains appear to have been sheared or elongated in an N-S direction. As a result of how dense the area is and because of the security challenges once faced by the people in and around the area, in-depth investigations towards tracing the likely occurrences of possible mylonites were not executed. These rocks were excavated for industrial purposes, probably for household finishings, tiles, or dimension stones, before being abandoned, leaving a massive opening that exhibits the degree of excavation that went on (Figures 16 and 17). These rocks were observed at Tashar na kwanar Gubuchi, the southern and southeastern parts of Gubuchi, at the boundary between Gubuchi, Turawa, Yarganji, and Yiryasa, amongst others. Rose Diagram showing the dominant trend direction of the fractures on the Porphyroblastic Gneiss to be NW-SE (Figure 18). This rock is coarse-grained and has both porphyroblasts and a well-developed fine-grained matrix. Petrographic studies showed that K-feldspar makes up about 30-35%, biotite is about 30-33%, quartz (19-25%), and plagioclase feldspar (5-9%). Accessory/opaque minerals account for about 4% of mineral composition (Figures 19 and 20). The porphyroblastic minerals were mostly K-feldspar.

Figure 15: Porphyroblastic Gneiss exposed at Gubuchi, Latitude 11° 13' 38"N and Longitude 08° 03' 52"E.

Figure 16: Massive exposure of Porphyroblastic Gneiss at Tashan na hawan Gubuchi; Latitude 11° 13' 38"N and Longitude 08° 03' 52"E.

Figure 17: Porphyroblastic gneiss highly rich in alkali feldspars and biotite. Latitude 11° 13' 38"N and Longitude 08° 03' 52"E.

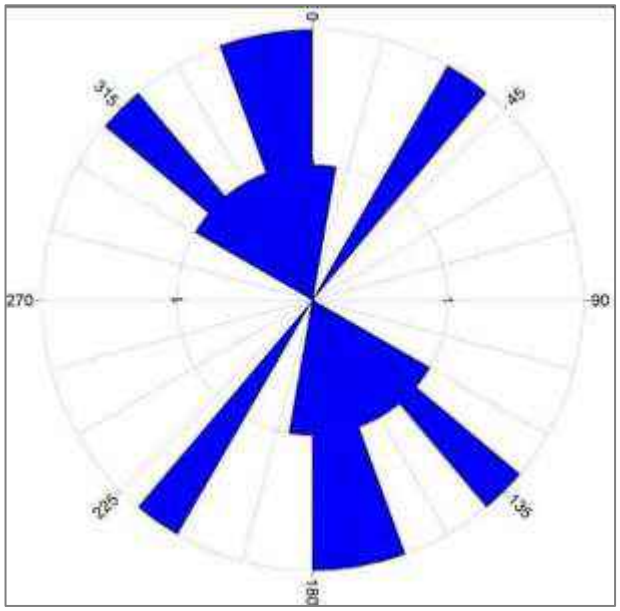

Figure 18: This rose diagram shows the dominant trend of the fractures on Porphyroblastic Gneiss to be NW-SE.

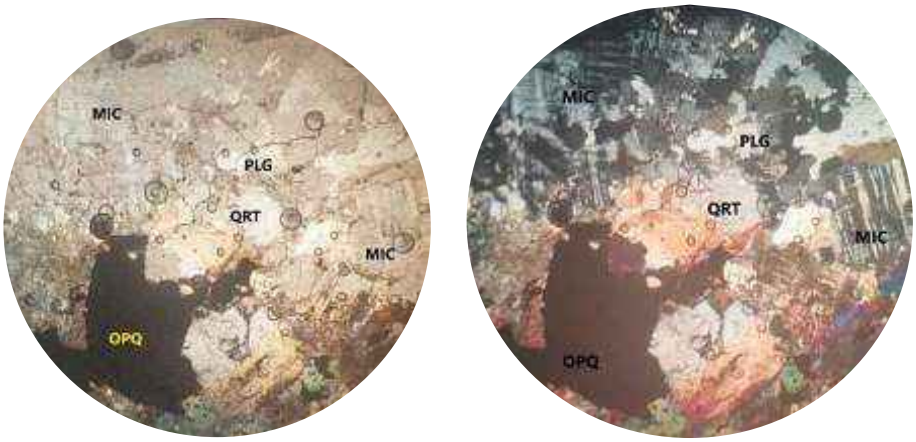

Figure 19: Photomicrograph of Porphyroblastic Gneiss under PPL (Left). Plate XX: Photomicrograph of Porphyroblastic Gneiss under XPL (Right). Microcline (MIC); Quartz (QRT); Plagioclase (PLG); Opaque Mineral (OPQ). Magnification (x40); Scale: 0.5mm.

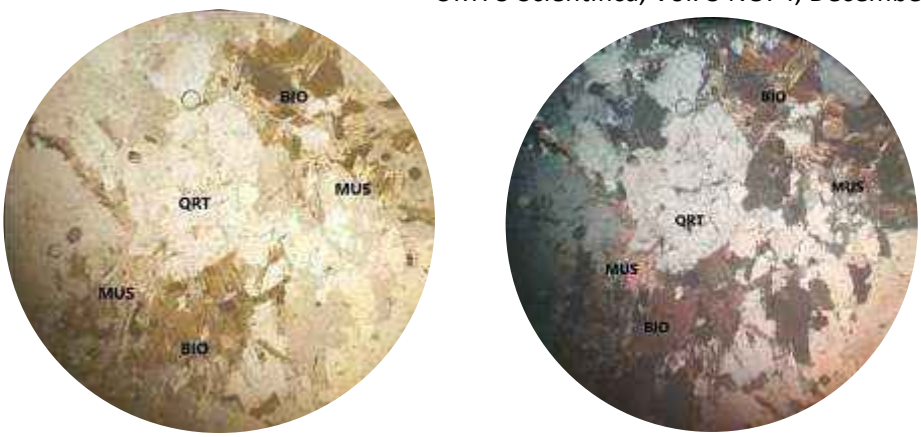

Figure 20: Photomicrograph of Porphyroblastic Gneiss under PPL (Left). Plate XXII: Photomicrograph of Porphyroblastic Gneiss under XPL (Right). Magnification (x40); Scale: 0.5mm. These plates show more of the Biotite (BIO) and Muscovite (MUS) with Quartz (QRT) metacrysts. This sample is different from that of the previous Figures but from the same rock type.

Medium-Coarse Grained Granite

These rocks (Figure 21) are found in the central regions of the study area and trend northwards. They are mostly weathered, and the mineral grains are medium to coarse-grained in size, predominantly made up of quartz, plagioclase and alkali feldspars, biotite, and opaque minerals, and they are a lot of unfilled joints, quartz and aplite veins of 0.8cm to 2cm wide, scanty appearance of pegmatitic dykes of about 19cm to 28cm wide. The pegmatites are mainly plagioclase and alkali feldspars, quartz, and biotite. These rocks are in contact with migmatitic gneiss, augen gneiss, granite gneiss, porphyroblastic gneiss, and porphyritic granite, which trend in an NW-SE direction and corresponds with the alignment of the mega fault that cross-cuts the study area, oriented in the same direction. At the contact with migmatitic gneisses within Safara Town, it was observed that this lithology exhibited some migmatitic foldings and foliations in some areas, a lot of fractures, joints (Figure 22), and faults (more sinistral than dextral faults) with displacements of about 5 to 11cm were observed. There were several quartzite ridges and pegmatites observed to have intruded this lithology. However, this lithology appears as packs of scattered boulders along the NW-SE fault zone and appears as tortoise backs in other locations. Rose Diagram was constructed from the strike readings of joints/veins/dykes and showed a dominant trend of NE-SW (Figure 23). Similar to field observations, the photomicrograph of medium-coarse-grained granite had about 43% of K-feldspar, plagioclase feldspar (10%), quartz (30%), and mica (17%). Several microfractures and micro-joints were observed cross-cutting mineral grains, and some were contained within a mineral grain. (Figure 24).

Figure 21: Medium-coarse-grained granite exhibiting some systematic joints in Mahangi; Latitude 11° 14' 38"N and Longitude 08° 15' 21"E.

Figure 22: Medium-coarse-grained granite at Mahangi; Latitude 11° 14' 38"N and Longitude 08° 15' 21"E.

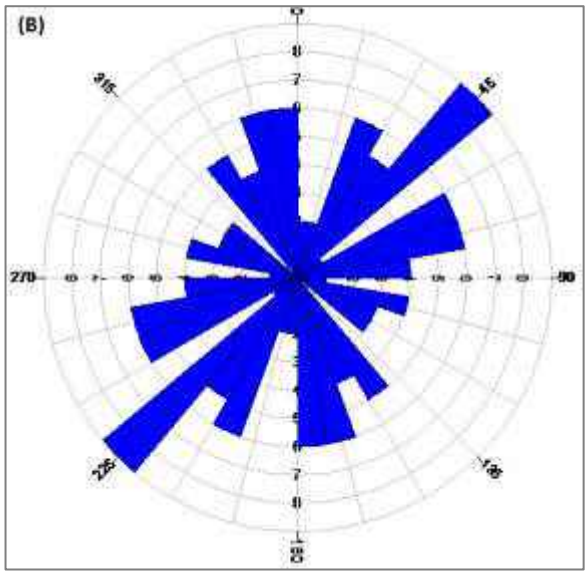

Figure 23: Rose Diagram constructed from the strike readings of fractures, showing a dominant trend of NE-SW.

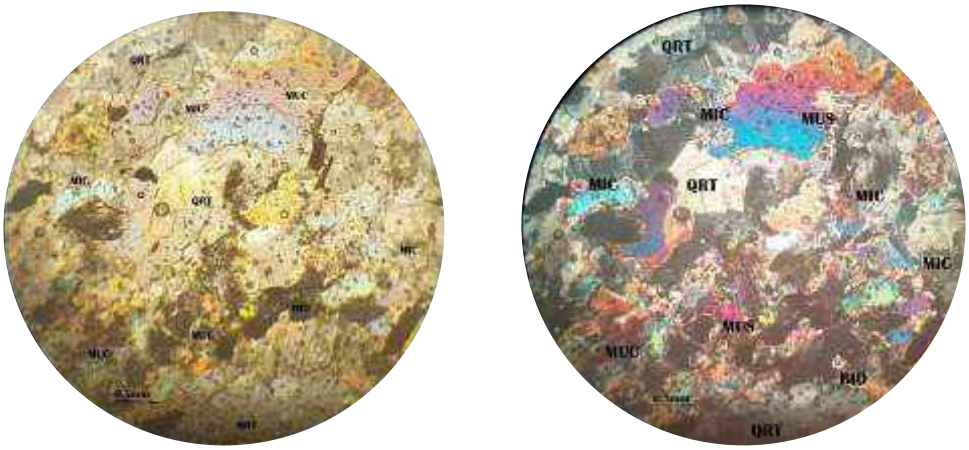

Figure 24: Photomicrograph of medium to coarse-grained granite in PPL (Left) and XPL (Right). Biotite (BIO); Microcline (MIC); Muscovite (MUC); Plagioclase (PLG); Quartz (QRT). Magnification (x40) and Scale (0.5mm).

Porphyritic Granite

These granitic rocks are made up of large mineral grains of plagioclase (white porphyritic granite) (Figures 25 and 26), and alkali (pink porphyritic granite) feldspars (Figures 27 and 28), quartz, biotite, and opaque minerals are smaller in grain sizes. They were identified as Ikara, Tudun Wada, Pala, Tiga, and Tsaya-Tsaya, amongst others. They mostly occur at fault and shear zones, and as such, they are affected by faulting and shearing, respectively. These rocks exist in the form of scattered massive and moderate-sized boulders, in the form of whalebacks, dome-shaped, steep, and gentle-edged hills, inselbergs, and mountainous formations. They are highly jointed and fragmented, have indentations, veins, and relicts of older rocks (xenoliths), and some of the boulders had parallel abrasions, which signified movement through a long distance. These rock units are oriented NW-SE, and very few are oriented NE-SW. Cataclastic rocks and discontinuous quartzite ridges intruded this lithology which are evidence of/signify fault zones. The porphyritic granite that was observed in Ikara exhibited lineations and sheared mineral grains (Figure 26). This zone was once reported to have undergone a minor earth tremor, and as observed, this zone lies exactly along the mega NW-SE fracture line. The rose diagrams (Figures 29 and 30) show the dominant trend direction(s) of lineaments measured from these porphyritic granites. The dominant trend was NW-SE. Cassiterite used to be mined from along the alluvial river channels. However, this work did not establish whether the cassiterite is of alluvial or pegmatite source.

Figure 25: Porphyritic granite (>plagioclase) in Tudun Wada; Latitude 11° 28' 11" N and Longitude 08° 20' 07" E.

Figure 26: Porphyritic granite (>plagioclase) exhibiting lineation in Ikara, along the NW-SE regional fault; Latitude 11° 10' 33" N and Longitude 08° 13' 37" E.

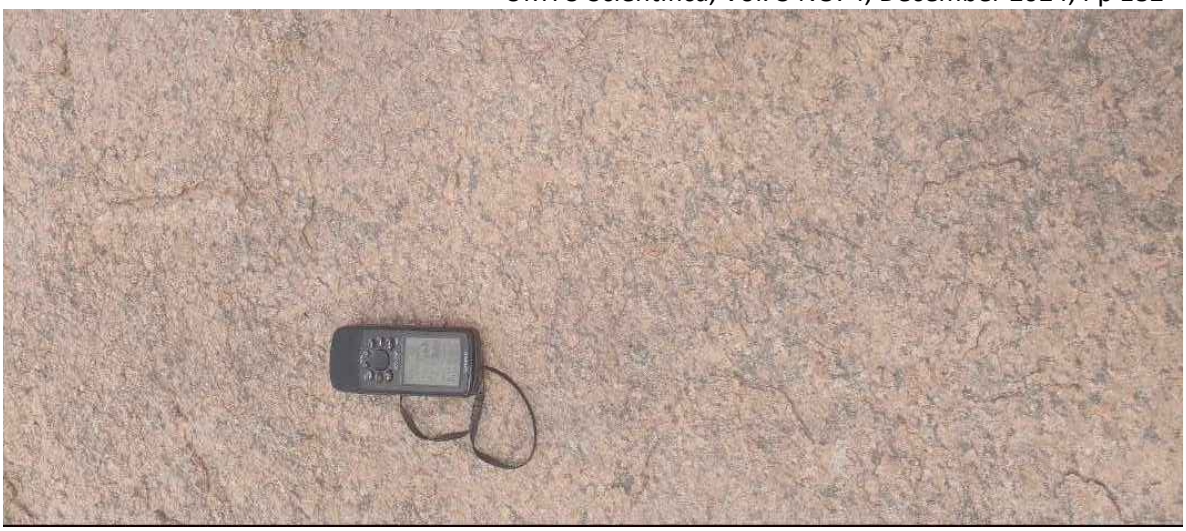

Figure 27: Porphyritic granite (>alkali feldspar) in Garin Rau; Latitude 11° 25' 22" N and Longitude 08° 16' 52" E.

Figure 28: Porphyritic granite (>alkali feldspar) showing medium to coarse grains of minerals in Garin Rau; Latitude 11° 25' 22" N and Longitude 08° 16' 52" E.

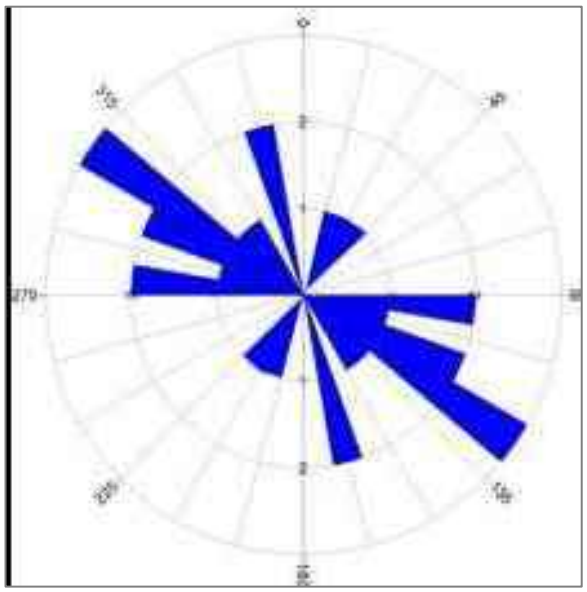

Figure 29: Rose Diagram constructed from the strike readings of lineaments within porphyritic granite (>alkali feldspar), showing a dominant trend of NW-SE.

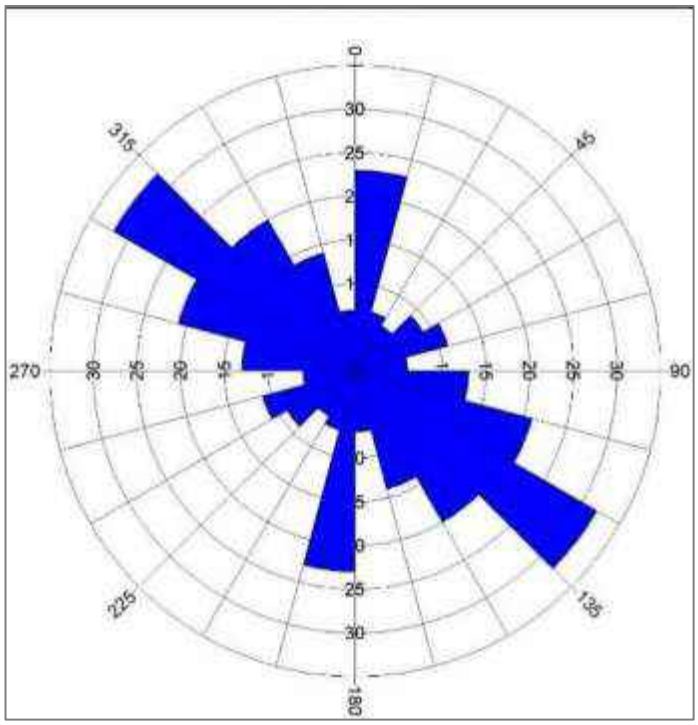

Figure 30: Rose Diagram constructed from the strike readings of lineaments within porphyritic granite (>plagioclase feldspar), showing a dominant trend of NW-SE.

Photomicrograph analyses of porphyritic granite under plane polarized light (PPL) and cross polarized light (XPL) were carried out. The minerals that form the phenocrysts were the K-feldspar in the pinkish porphyritic granite, and plagioclase feldspar were the phenocrysts in the whitish porphyritic granite, though few large crystals of quartz were found. In the Porphyritic granite (>alkali feldspar), the dominant minerals were the K-feldspar of about (35%), plagioclase feldspar (30%), quartz (20%), biotite (10%), muscovite (3%) and some opaque minerals (2%) (Figure 31). The opaque minerals (OPQ) are possibly magnetite and zircon. Whereas the porphyritic granite with dominant plagioclase feldspar is about 40% rich, quartz (26%), alkali feldspar (16%), biotite (9%), muscovite (5%), accessory minerals (4%) (Figure 32).

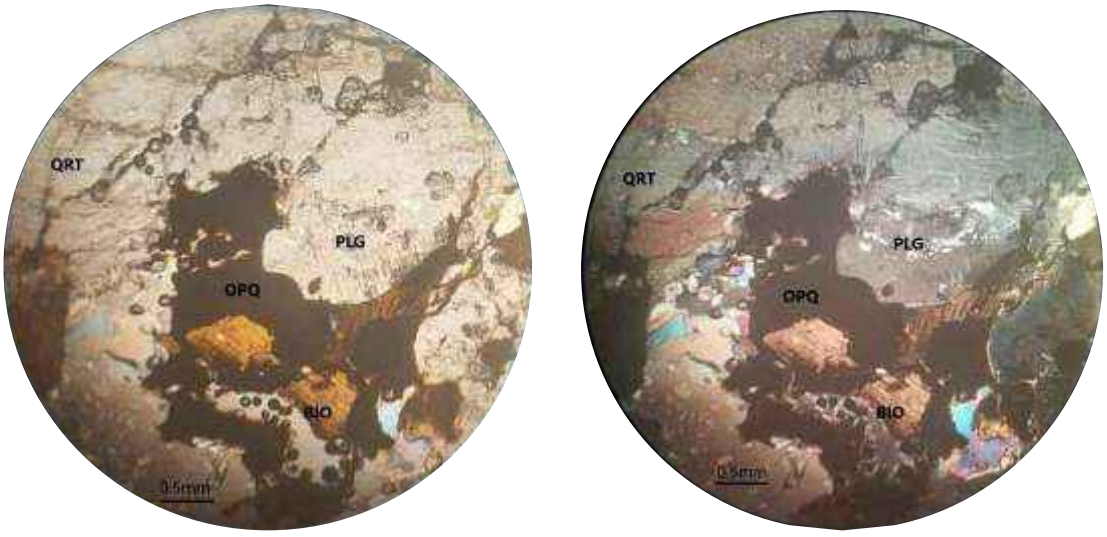

Figure 31: Photomicrograph of porphyritic granite (>alkali feldspar) in PPL (Left): in XPL (Right). Magnification (x40) and Scale (0.5mm). Micro-pods and intragranular mineral grains of quartz within alkali feldspar and quartz.

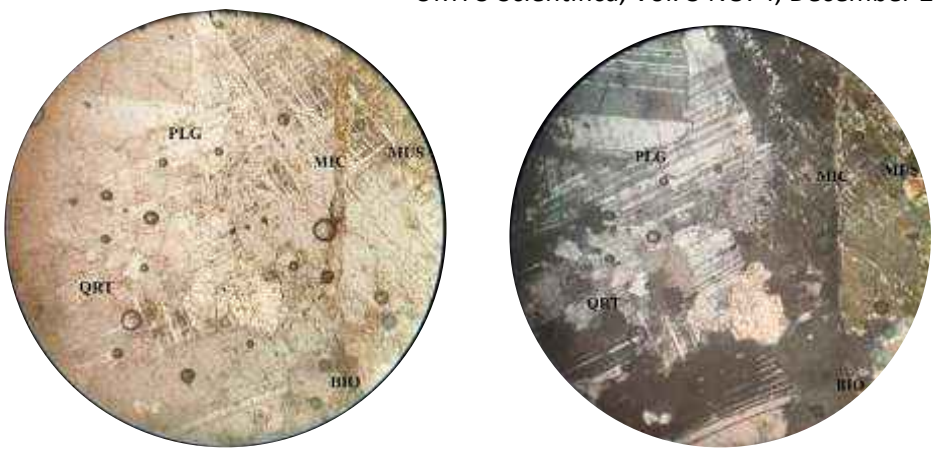

Figure 32: Photomicrograph of porphyritic granite (>plagioclase feldspar) in PPL (Left); in XPL (Right). Biotite (BIO); Microcline (MIC); Muscovite (MUC); Orthoclase (ORT); Plagioclase (PLG); Quartz (QRT). Magnification (x40) and Scale (0.5mm).

Quartzite

Quartzites are most times used as indicators to identify fault and shear zones. These were observed in several localities orienting 120° to 178° NW-SE, dipping 43° to 61° SW, and 014° to 30° NE-SW, dipping 18° to 58° SE. Some of these ridges were aligned laterally beside one another about 15 to 25 meters apart in a discontinuous pattern (Figure 33). They are in the form of hills ridges and have several scattered cobbles and boulders surrounding the ridges. They cross-cut the granitic and gneissic rocks. Some of the quartzites are mylonitized (quartz-mylonites) and host amethyst mineralization within them. These highly sheared quartzites are trending almost N-S. This is an indication of syn-tectonic events and different stress regimes that gave rise to the changes in the orientation of the rocks and structures in that area. (Figure 34 "a and b"). Most of these quartzites were lateratized, and some scattered pieces of hollow blackish-red rocks (in the form of "box-works") were also identified. Low quartzite ridges and quartzite boulders were scattered around in large and small pieces, while some were cumulated. Figure 35 is a Rose Diagram that shows the directional trend of fractures from the rock. The thin section of this rock shows the dominant mineral of quartz of about 97% quartz of anhedral and brecciated form. The quartz was affected by intergranular and intragranular fracturing (Figure 36). Other minerals observed are feldspar and mica making up about 3%.

Figure 33: Quartzite ridges located at Latitude 11° 13' 31" N and Longitude 08° 15' 00" E (Gidan Kare area).

Figure 34. a: Mineralized veins that host amethyst at Longitude 11° 13' 33" N and Longitude 08° 13' 51" E. b: Hand sample of quartzite with traces of amethyst (Gidan Kare area).

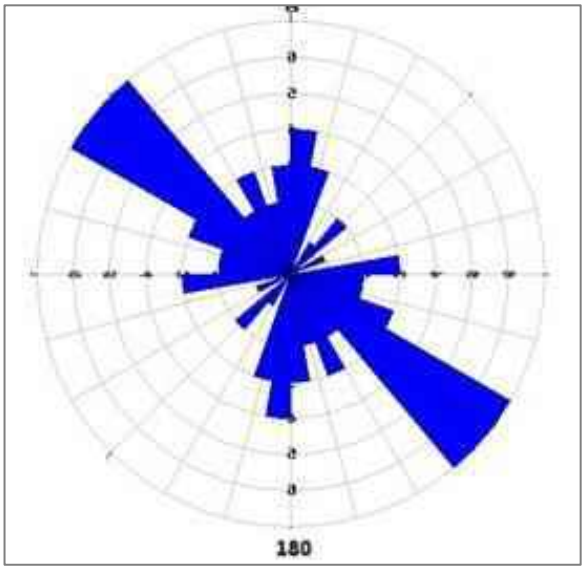

Figure 35: Rose Diagram depicting the major trend (almost N-S) of the fractures recorded from the quartzites.

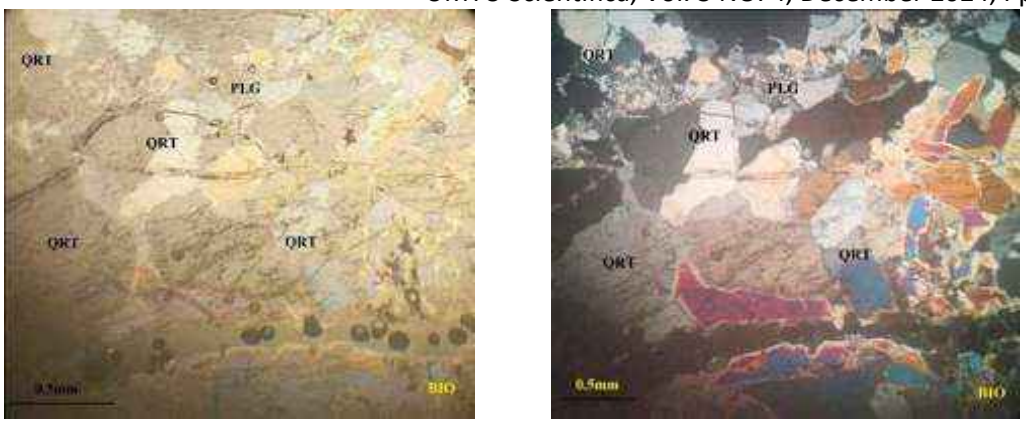

Figure 36: a: Photomicrograph of quartzite in PPL (Left); b: Photomicrograph of quartzite in XPL. Quartz (QRT) and Plagioclase (PLG). Magnification: x40; Scale: 0.5mm

Pegmatites

Pegmatites (Figure 37) occur mostly within the gneissic lithologies, especially within the granitic gneiss and migmatitic gneiss. Few were observed within the porphyritic granites and medium to coarse-grained granites. These lithologies are often dome-shaped and in the form of whalebacks trending NW-SE, NE-SW, and N-S. The thickness of pegmatites varies from a few centimeters to several meters as veins and dykes, with dimensions ranging from 1.5cm to 47.6cm. Some of the pegmatites extend for several meters, ranging from 3m to 10m. They are composed of large quartz, alkali, and plagioclase feldspars and mica (biotite and muscovite) that are over 10 cm wide. The pegmatites in porphyritic granites observed along the river channel at Mahangi MAY BE the source of cassiterite. Due to the high level of weathering of these categories of pegmatites, fresh samples were difficult to obtain. The pegmatites extend for several meters across the porphyritic granites. Table 1 shows the summary of the mineralogical compositions of the lithological units found within the study area" after the last sentence under Pegmatites

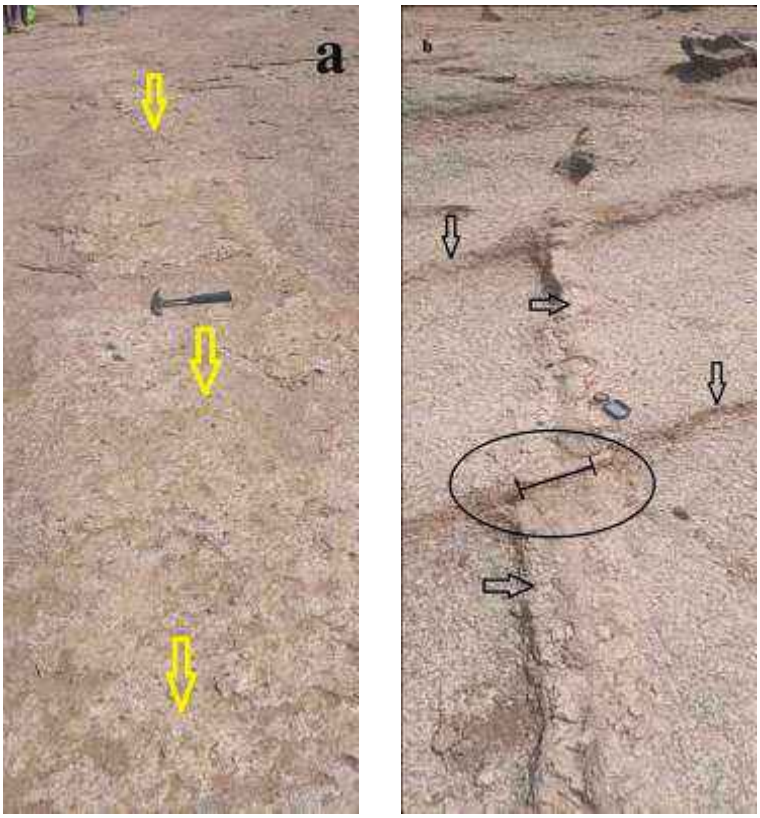

Figure 37: a: Pegmatitic dyke in porphyritic granite at Ikara (Latitude 11° 10' 33" N and Longitude 08° 13' 37" E). Arrows and outlines showing the pegmatite and its width; b: Coarse-grained pegmatite (shown by right-pointing arrows) cross-cut by systematic joints (downward arrows) and displaced dextrally (oval and outline indicating displacement) in porphyritic granite found at Tudun Wada (Latitude 11° 16' 02" N and Longitude 08° 20' 46" E).

Table 1: Summary of the mineralogical modal compositions of the minerals identified from the individual rock types

	MINERALS IN PERCENTAGE (%)								
Rocks	**BIO**	**GAR**	**HRN**	**MIC**	**MUS**	**OPQ**	**ORT**	**PLG**	**QRT**
Migmatitic Gneiss	27	0	3	14	0	2	0	34	20
Migmatitic (Augen) Gneiss	26	0	2	13	0	3	0	35	21
Granite Gneiss	26	0	0	15	2	2	0	30	25
Porphyroblastic Gneiss	31	0	0	22	1	4	11	8	23
Medium-Coarse Grained Granite	15	0	0	36	2	0	7	10	30
Porphyritic Granite	10/10	0/4	0	35/16	3/4	2/0	0	30/40	20/26
Quartzite	1	0	0	0	0	0	0	2	97
Pegmatite	13	0	0	0	0	0	8	19	60

BIO: Biotite; GAR: Garnet; HRN: Hornblende; MIC: Microcline; MUS: Muscovite; OPQ: Opaque Minerals; ORT: Orthoclase Feldspar; PLG: Plagioclase Feldspar; QRT: Quartz

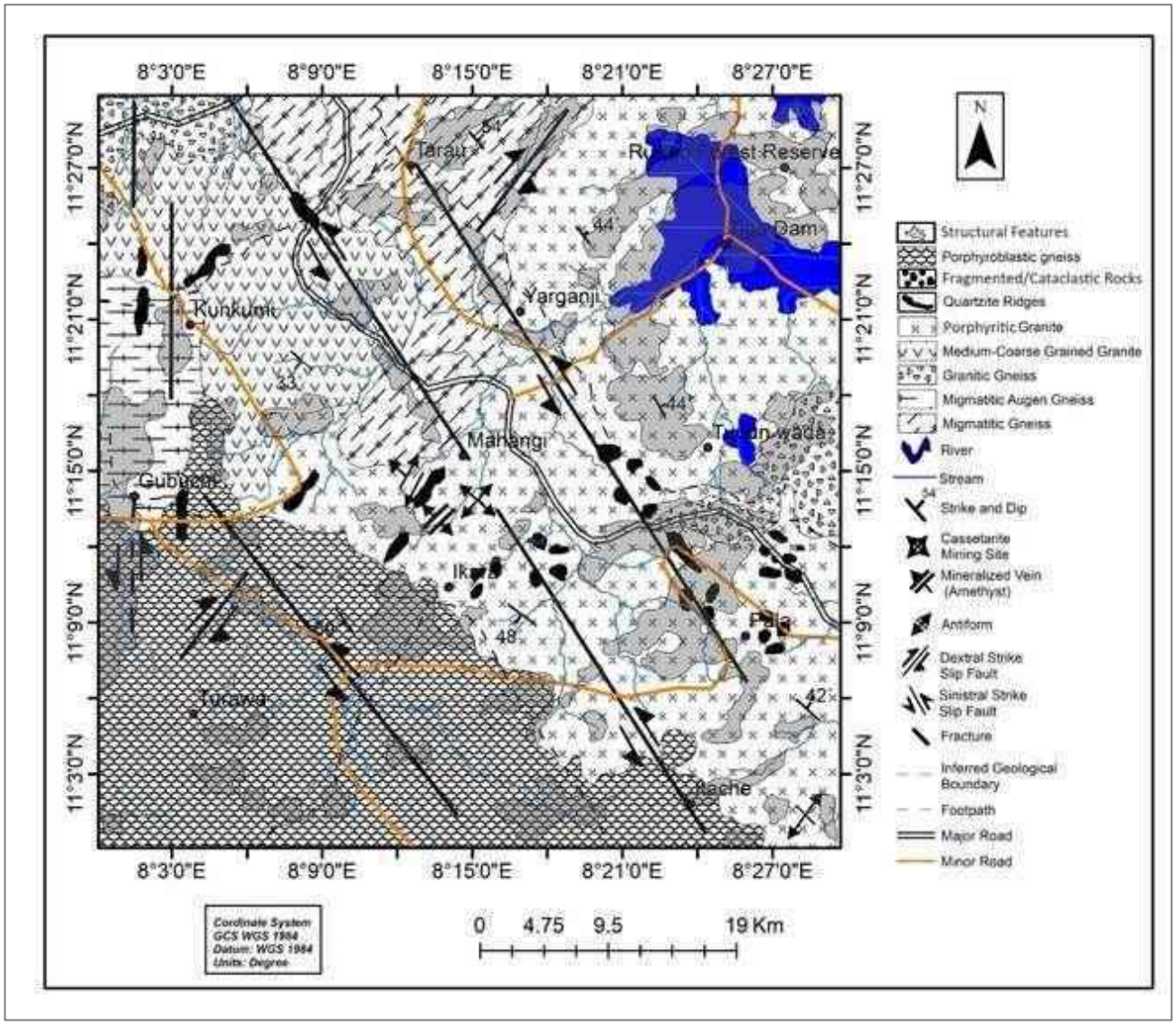

Figure 38: Litho-structural map of the study area with major regional fractures and other structural features shown, on a scale of 1:100,000

STRUCTURAL DESCRIPTIONS

There were several landforms and structural features observed on the outcrops during fieldwork. Below are some seen and described with their characteristics:

Joints

These are tensile fractures caused by extensional stress where no displacement is seen. They are usually oriented parallel to σ_1 and perpendicular to σ_3, and these cracks or fissile structures open horizontally while extending

vertically. These brittle structures can extend from a few millimeters (micro-joints) and centimeters to several meters to kilometers, depending on the extent of the lithology, and are either syn-tectonic or post-tectonic. The gneisses and migmatites-gneisses exhibited more joints than the granitic rocks that are because the metamorphic rocks are stiffer and have more closely spaced joints than the granitic rocks (Harris *et al.,* 1960; Ladeira and Price, 1981). Some of them are empty, while some are filled with one or more minerals such as monomineralic, di-mineralic, or polymineralic veins, pegmatitic veins, and pegmatitic dykes. They exhibit different patterns but the ones observed within some lithologies in the study area were more of systematic, non-systematic joints and penetrative joints. The systematic joints (Figure 39) have regular spacings and orientation; non-systematic (Figure 40) joints have irregular spacings and orientation; and penetrative joints (Figure 41) deeply cut across some lithological units horizontally, which have similar characteristics as bedding joints exhibited within layered sedimentary rocks. The trends of the joints, veins, and dykes are NNW-SSE, NNE-SSW, NW-SE, NE-SW, N-S, and E-W.

Figure 39: Photograph of systematic joints on Medium-coarse grained granite at Mahangi. Latitude 11° 14' 38" N and Longitude 08° 15' 21" E.

Figure 40: Photograph of non-systematic joints on Porphyritic granite (>alkali feldspar) at Garin Rau. Latitude 11° 25' 22" N and Longitude 08° 16' 52" E.

Figure 41: Photograph of penetrative joints through porphyroblastic gneiss at Tashan na hawan Gubuchi; Latitude 11° 13' 38"N and Longitude 08° 03' 52"E.

Faults

These are fractures, a type of brittle deformation caused by tensional stress but different from joints in that the faults show displacements of rock units in the study area. Faults are developed from the strike-slip displacement of joints, veins, and dykes in the field. Strike-slip faults were identified more in the gneissic rocks compared to the few seen on granitic rocks. The offset makers which are mostly veins and dykes are displaced either to the left (sinistral) (Figure 42) or to the right (dextral) (Figure 43). However, these faults vary in displacement lengths, widths of the fault planes and offset makers, and varying degrees at which the offset makers and fault planes trend. It was observed that some fault planes on the granites trend in NE-SW direction while the displaced veins and dykes are oriented NW-SE. The displacement of the veins and dykes along the fault planes was 3.5cm to 10cm. The trend values of the fault planes were between 009º-086º (NE-SW). The displaced veins and dykes within the gneissic rocks have strike values between 251º-339º (NW-SE) and dip readings between 17º-24º (SE) at the north-western part of the study area. Within granitic rocks, strike values were between 010º-029º (NE-SW), and the dip readings at 19º-22º (SE). The joints that evolved first are classified as D_1; the veins and dykes are D_2, and the fault displacements are D_3.

Figure 42: A sinistral strike-slip fault at Gangarida area; Latitude 11° 23' 50" N and Longitude 08° 05' 58" E.

Figure 43: A dextral strike-slip fault at Gangarida area; Latitude 11° 23' 50" N and Longitude 08° 05' 58" E.

Veins and Dykes

Veins and dykes are discordant intrusive structural features formed from hydrothermal fluids which fill in joints and vary in widths and lengths. These were commonly observed within the gneisses and granitoids of the study area. The veins are narrower, not more than 10cm. They are joints that became filled with minerals, cross-cutting each other or seen as a singular body. A series of cross-cutting (diadysites) monomineralic (quartz or calcite), di-mineralic (quartz and feldspar), and polymineralic veins (pegmatitic or aplite veins) were observed across most of the gneissic lithology and fewer on medium-coarse grained and fine-grained granite outcrops (Figure 44 and 45). Dykes are wider than veins; they are also once-upon-a-time joints that eventually get filled by more than one mineral. They occur mostly as pegmatitic dykes and extend from a few centimeters to about 50 meters (depending on the broadness of exposure). Both veins and dykes were observed to be displaced at points by younger joints. Displacement was either dextrally or sinistrally (as seen in Figures 42 and 43 above). These younger joints are unfilled, while some are filled with one mineral or more.

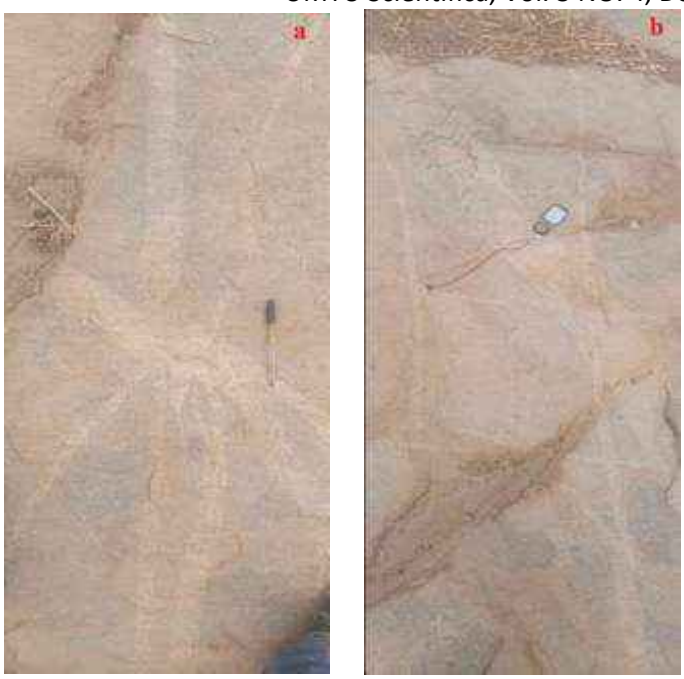

Figure 44 "a and b": Veins on granite-gneiss at Ungwan Gangarda; Latitude 11° 23' 50"N and Longitude 08° 05' 58"E.

Figure 45: Dykes on porphyritic granite (a): Latitude 11° 10' 33" N and Longitude 08° 13' 37" E and on granite-gneiss (b) Latitude 11° 23' 50"N and Longitude 08° 05' 58"E

Folds

Folds are ductile deformations formed as a result of compressional stress acting perpendicular to the axial plane of a fold. Most of the features folded, as observed in the field, were quartz veins, pegmatitic veins, pegmatitic dykes, and foliations of gneisses. The types of folds seen were: chevron symmetric fold (70°-120°) exhibited by pegmatitic dykes and veins (based on an interlimb angle) on gneisses and fine-grained granite (Figure 46); chevron (symmetric fold) (based on fold style/shape) exhibited by fine-grained mineral alignment of migmatitic-gneiss (Figure 47); and ptygmatic folds (based on the mechanics of origin and internal kinematics) exhibited by quartzo-feldspathic minerals across a xenolith of porphyritic granite that intruded a migmatitic-gneiss (Figure 48). Migmatitic-gneisses are on the verge of igneous rock formation. Thus foldings exhibited by light and dark-colored minerals are very common and typical characteristics of mixed rocks. Features like "piecemeals" were seen exposed in a lot of parts on the migmatitic-gneisses.

Figure 46: Open angle fold (70°-120°) exhibited by pegmatitic dykes and veins (based on interlimb angle) on granite-gneiss; Latitude 11° 23' 49"N and Longitude 08° 05' 55"E.

Figure 47: Chevron symmetric folds (based on fold style/shape) exhibited by fine-grained mineral alignment of migmatitic-gneiss; Latitude 11° 29' 15" N and Longitude 08° 13' 01" E.

Figure 48: Ptygmatic folds (based on the mechanics of origin and internal kinematics) exhibited by quartzo-feldspathic minerals across a xenolith of porphyritic granite that intruded a migmatitic-gneiss; Latitude 11° 29' 20" N and Longitude 08° 13' 41" E.

Foliations and Lineations

Foliations (Figure 49) are planar surficial/penetrative structures that are homogeneously distributed on metamorphic rocks exposed in the study area with varying widths. They are defined by the parallel alignment of flattened mineral grains of alternating light and dark color minerals as bands. The foliations identified are exhibited by the varieties of gneisses observed in the field. They are made up of parallel planar alignments (compositional bandings) of quartz and feldspars (plagioclase and alkali feldspars), which make up the light-colored bands, and the mafic minerals (e.g. biotite, garnets, hornblende) making up the dark bands. The word "banded" is used with a few millimeters spacing, and this is known as "gneissic foliation, gneissic banding, or gneissosity" and are distinctive features of gneissic and migmatitic rocks. Irrespective of the flow structures exhibited by migmatites, the compositional bandings are still eminent. There are several joints, veins, and dykes that cross-cut these foliations, and as such, it can be suggested that the foliations formed first as S_1, then the joints as D_2, followed by the discordant structures (veins and dykes) as D_3. Lineations (Figure 50) are linear structures characterized by the homogeneous superficial arrangements of some mineral grains in a certain order that developed on the

surface of the rock exposure. These were observed clearly on the porphyritic granites at the zone where there was a minor earth tremor some years ago in Ikara LGA. The minerals exhibiting this feature are quartzo-feldspathic. The foliations identified on migmatite-gneisses are primary structures because they were formed during the formation of the rocks, while those lineations identified on porphyritic granites are suggested to be secondary structures because they are non-penetrative and those penetrative lineations identified on porphyritic granites are also suggested to be primary structures.

Figure 49: Gneissic banding/foliation exhibited on Migmatitic gneiss at Latitude 11° 29' 15" N and Longitude 08° 13' 01" E.

Figure 50: Porphyritic granite (>plagioclase feldspar) exhibiting magmatic lineation at Ikara, along the NW-SE regional fault; Latitude 11° 10' 33" N and Longitude 08° 13' 37" E.

Xenoliths

These were country rocks that ended up being embedded or encircled in a larger rock mass through the development and solidification of a later rock. These were features observed within the porphyritic granites and granite-gneisses. They mostly represent parts or remains of an older rock that got incorporated within the magma before the solidification to form a new, younger rock. Most times, they are related to the younger rock and also not too far in proximity to where it originally lies (Figure 51).

Figure 51: Porphyritic granite (>plagioclase feldspar) appearances of xenoliths at Tudun Wada; 11° 28' 11" N; 08° 20' 07"E.

Shear Zone

Shear zones are observed at the extreme western and at the eastern parts of the study area. Towards the west, the shear zone affected the migmatitic (augen) gneisses, while towards the east, the lithologies affected by the extensional shear stress are the porphyritic granites (Figure 52). Both shear zones were oriented N-S and were both cross-cut by the regional NW-SE fault. The shear zones have rocks that have undergone shear stress (dynamic recrystallization), exhibited by the elongation of mineral grains. Porphyritic granites, migmatitic (augen) gneiss and porphyroblastic gneisses were affected by shear stress. Porphyroblastic/augen mineral grains in rocks became lenticular/elongated with boudins. These rocks can be said to be mylonitized, as the mineral grains have been milled. The shear zones in the study area are hybrids in that both brittle and ductile deformations exist in the shear zones. Brittle deformations, e.g., fracturing, faulting, brecciation, rock pinnacles, and cataclastic fault rock/fragments, are seen within the shear zone and thus can be called brittle-ductile shear zones. Photomicrographs of samples taken show shearing of mineral grains exhibiting mylonitic fabric with brittle features such as micro-faults, micro-fractures, and micro-breccias (Figure 53). This means that ductile and brittle deformations affected the rock, as seen exhibited by the mineral grains.

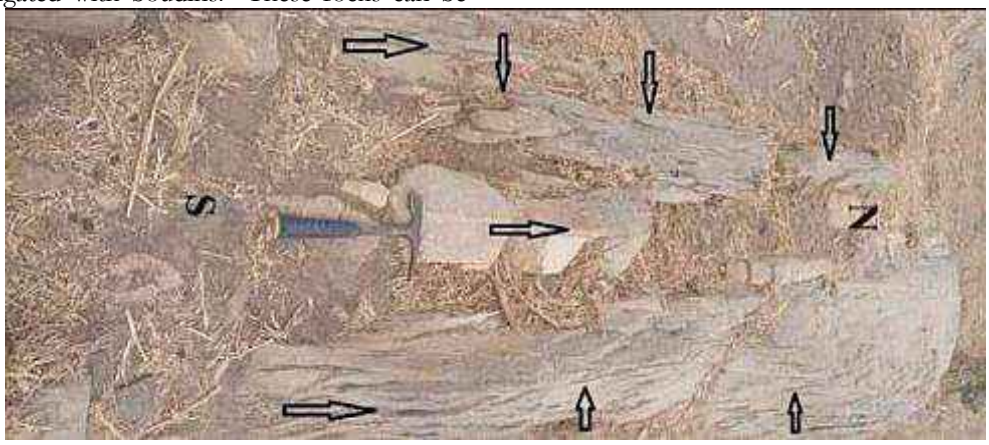

Figure 52: Part of migmatitic (augen) gneiss in the form of sheared pinnacles in an N-S trending shear zone; Latitude 11° 21' 57" N and Longitude 08° 02' 31" E.

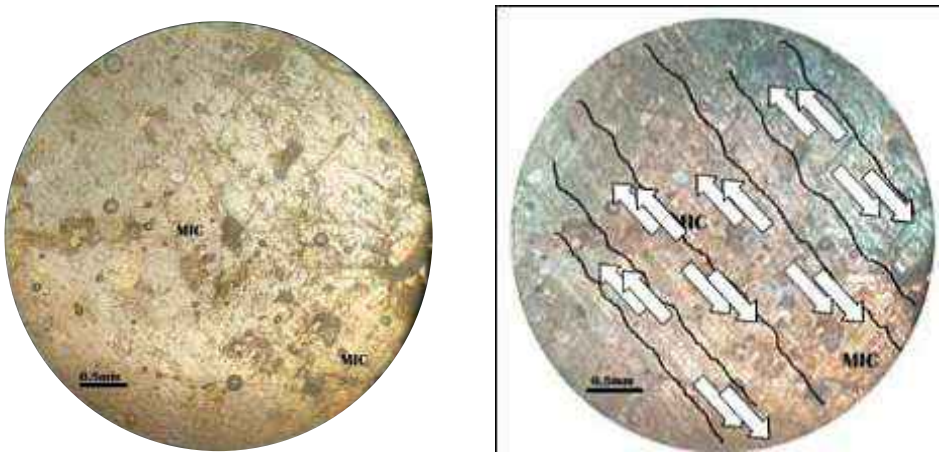

Figure 53: Photomicrographs (in PPL and XPL) of a sheared gneiss observed under the microscope. The XPL view (right) shows the aftermath of shear stress (further extensional pull) upon the microcline. Magnification: x40; Scale: 0.5mm.

MICROSTRUCTURES

Several microstructures were observed from the thin section analysis of rock samples taken from the field. These microstructures were formed due to both brittle and ductile deformation processes and reflect the structures that formed on a large scale. These were identified across and between minerals observed in the thin section slides. Deformations such as fractures (joints and faults), folds, foliations (banding), etc., occurred due to some environmental factors, namely temperature, fluid and litho-static pressure, differential stress, and the aftermath (i.e., strain) is what was produced as structures. Hence, the microstructures that eventually formed were used to suggest the deformational events that had taken place. Mineral grains of either the same or different characteristics/forms were separated from one another by grain boundaries, thus suggesting that each mineral had a

specific lattice orientation or crystallographic arrangement. Some microstructures had undergone several stages of deformations before their current final form. However, some of the ones identified include signature microstructures that depicted atomic lattice deformations, i.e., their current form is what was formed after stress had affected the atomic lattice.

Micro-fractures

These were elongated or small, narrow, linear, or curvi-linear cracks that cut through mineral grains (intragranular fractures) or transgressed across several grains (intergranular fractures). There were micro-joints and micro-faults observed from thin section slides. These microfractures were not in a systematic nor uniform order/orientation. It was observed that in some of the slides, mineral grains like the quartz filled up some of these openings and, thus, were like micro-veins. Microfractures that exist in this manner are referred to as "healed" microfractures. Thus, this phenomenon inhibits further extensions or elongations of an existing fracture(s) perpendicular to the healed microfracture(s). However, some of these microfractures curved away from the healed microfractures but eventually got terminated. It was also observed that finer fragments of mineral grains were formed along fractures and these types of fracturing are termed trans-granular fracturing through the process termed constrained comminution. Figure 54 shows micro-joints and micro-faults.

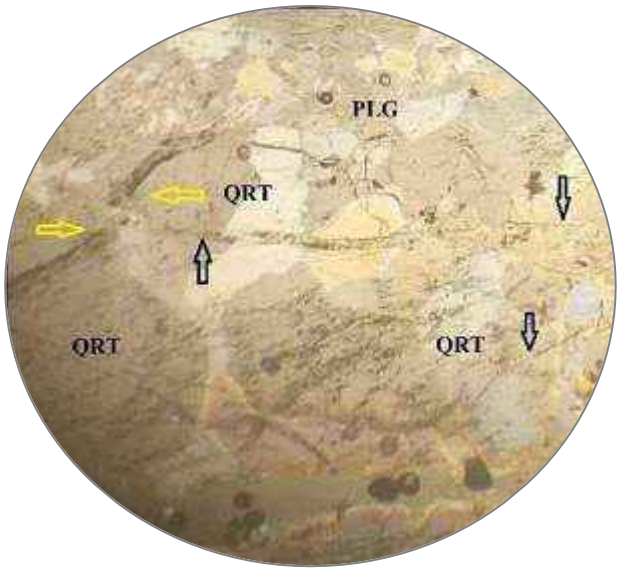

Figure 54: A quartzite showing micro-joints (black arrows) and micro-fault of a micro-vein displaced sinistrally (yellow arrows).

Micro-foliations

Micro-foliations are linear alignments of the same or different mineral types. They are ductile penetrative microstructures in which maximum stress acts perpendicular to the layers of minerals. Some of these micro-foliations appeared in a wavy pattern/form. Gneissic foliation was observed from the gneissic rocks and is also referred to as "gneissic bandings". The gneissic rocks exhibit this microstructure. However, mylonitic foliation is another type of foliation that was identified from sheared rocks (migmatitic (augen) gneiss and porphyroblastic gneiss), indicating the direction of shear. For the case of the sheared foliated rocks, maximum shear stress acted parallel to the layers (plastic deformation) after the principal stress had acted perpendicularly to the plane of mineral grains. Figure 55 shows micro-foliations in the form of gneissic bandings.

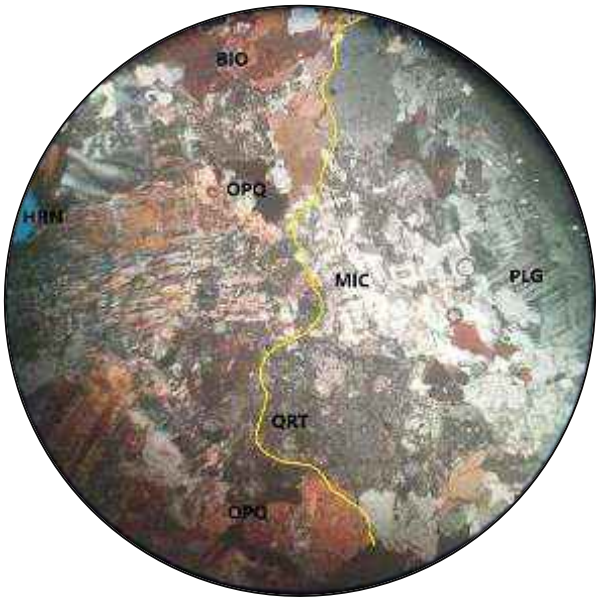

Figure 55: Micro-foliation exhibited in migmatitic gneiss.

Myrmekites

Myrmekite (Wartlike myrmekite) microstructures are intergrowths of quartz that were identified within some feldspar and quartz mineral grains. These were wormy, vermicular features exhibited by quartz as intergrowths. These possibly formed during cataclastic and/or shear tectonic activities which gave rise to tectonic strains and resulted in the formation of fractures within the minerals. These fractures were filled up by smaller quartz grains. Stress caused the nucleation of these myrmekites along interfaces, already characterized by elastic strain stored within the quartz grains. Figure 56a shows wormy-like myrmekites. In addition, mineral inclusions of zircon grains were observed within larger quartz minerals (Figure 56b). Micro-veins were also identified across some quartz grains. These were once joints that eventually got filled by granular quartz minerals in the form of micro-pods.

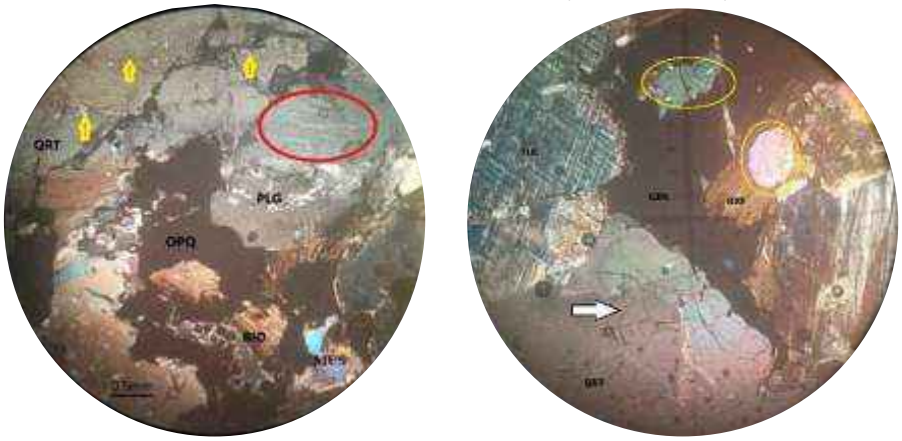

Figure 56: a: Photomicrograph of porphyritic granite showing wormy-like myrmekites circled in red, with the presence of micro-veins (yellow arrows); b: mineral inclusions of zircon mineral grains found within larger quartz minerals (yellow ovals); and micro-cracks (white arrow). (Quartz (QRT); Microcline (MIC); Biotite (BIO); Garnet (GRN))

Micro-folds

A series of folds were seen exhibited on rocks, which were caused by compressional stress. These ductile deformations were observed mostly within the gneissic rocks within shear zones along the regional faults. And as such, they are representative structures of those formed at the micro scale. Therefore, these micro-folds identified during microstructural analyses formed as a result of mineral grains that had undergone ductile deformation (Figure 57).

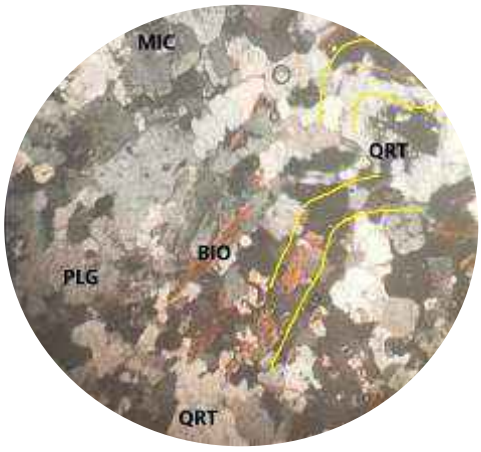

Figure 57: Showing micro-folding of biotite in a sheared zoned underlain by migmatitic (augen) gneiss.

Granoblastic and Porphyroblastic Textures

Some metamorphic rocks observed within the study area display granoblastic and porphyroblastic textures. Quartzites exhibit the granoblastic texture while the porphyroblastic texture is displayed by the migmatitic (augen) gneisses and porphyroblastic gneisses (Figure 58 "a and b"). This signified a delay in the formation of the large mineral grains as they took time before the final formation within the melt. The granoblastic texture is a non-foliated fabric where the mineral grains are not aligned. The porphyroblastic texture has large mineral grains surrounded by the finer grain matrix within a foliated rock.

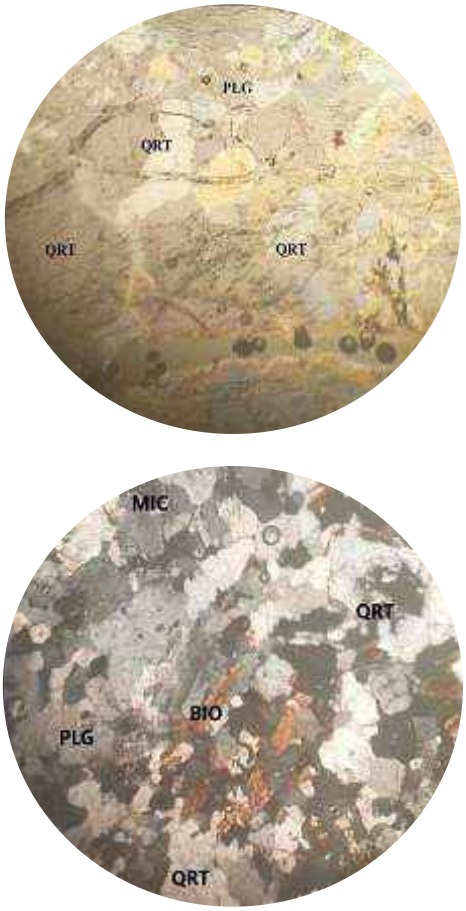

Figure 58: a: (UP) showing a granoblastic texture exhibited by quartzite; b: (DOWN) showing the porphyroblastic texture (large quartz mineral grains within the small matrix of other minerals) in a migmatitic (augen) gneiss.

Land-forms

In the field, rocks were exposed in various forms regarded as landforms. Igneous and metamorphic rocks identified during the field study exhibited similar or varying forms. The landforms in which these lithologies appear in the field are dome-shaped, whale-backs, ridges, hills, rock fragments, and boulders (Figures 59 to 64).

Figure 59: Dome-shaped medium to coarse-grained granite at Ungwan Sarkin Zaki; 11° 14' 38"N; 08° 15' 21"E.

Figure 60: Low to moderate laying whale-back of migmatitic-gneiss at Bebeji; Latitude 11° 28' 55" N and Longitude 08° 13' 00 "E.

Figure 61: Discontinuous quartzite ridges at Kunkumi; Latitude 11° 13' 12" N and Longitude 08° 13' 36"E.

Figure 62: Quartzite hills at Gidan Kare area; Latitude 11° 13' 33" N and Longitude 08° 13' 39" E.

Figure 63: Highly lateratized boulders at Kunkumi axis; Latitude 11° 21' 50" N and Longitude 08° 02' 27" E.

Figure 64: Massive intrusive hills at Pala; Latitude 11° 08' 30" N and Longitude 08° 27' 00" E.

CONCLUSION

The study area was mapped on a scale of 1:100,000 and underlain predominantly by gneisses and granite varieties, with occurrences of quartzites and pegmatite intrusions. The evolution of these gneissic and granitic lithologies can be traced from the Archean to the Pan-African. However, the gneissic rocks were formed at great depths where the temperature and pressure conditions are so high, and as such, classified under Barrovian Facies (Eskola, 1963; Saggerson and Turner, 1972; Bucher and Frey, 2002). The structural features like the fractures (joints and faults), foliations, lineations, and pieces of evidence of shearing were formed during (syn-tectonic) and after (post-tectonic) rock formations, spanning to the late Pan-African orogeny. The fractures have a dominant trend towards the NW-SE. Few were trending NE-SW, N-S, WNW-ESE, and E-W. This shows thatearlier formed structures, (WNW-ESE and E-W) evolved during the Eburnean/Kibaran orogenies, and were superimposed by the late Pan-African structures (NW-SE, NE-SW, and N-S). However, there are superficial deposits over some

lithological exposures caused by weathering and erosional effects.

ACKNOWLEDGMENT

To the good people of Gubuchi, Kunkumi, Mahanji, Tarau, Tiga, Tudun Wada, Dankade, Ikara, Pala, Gajale, Ikara, Ungwan Sarkin Zaki, Gidan Kare, Makarfi, Kiru and Bebeji LGAs of Kaduna and Kano States, that aided me and permitted me to do my work, may Allah bless and reward you, amen. I thank Mal. Yusuf Gangara for using his car and securing a motorcycle, which was used to navigate both motorable and non-motorable places.

CONFLICT OF INTEREST

There was no conflict of interest whatsoever between the authors.

REFERENCES

Abdulhamid, N. T., 2017. Geology, Geochemistry and Structural Controls of Badafi Pegmatite Field, Parts of Sheets 80 (Kabo SW, SE) and Sheet 103 (Ikara NW, NE), Northwestern Nigeria *(Unpublished MSc. Thesis). Ahmadu Bello University, Zaria.*

Abdulmalik, N. F., 2016. Geology and Tectonic History of the Basement Complex Rocks in Shanono Area, Part of Sheet 56 (Musawa SE), Northwestern Nigeria. *An M.Sc. Dissertation, Geology Department, Ahmadu Bello University, Zaria.,* 128 pages.

Abdulmalik, N. F., Garba, I., Danbatta, U. A. and Hamza, H., 2018. Delineation and Correlation of Lineaments Using Landsat-7 ETM+, DEM and Aero-magnetic Datasets: Basement Complex of Shanono, Northwestern Nigeria. *Journal of Geology and Geophysics,* 7:4 **[Crossref]**

Abdulmalik, N. F. and Umaru, A. O., 2020. Interpretation of Aeromagnetic and Aero-radiometric Data in Delineating Major Fractures within Sheet 56 (Musawa SE), Northwestern Nigeria. *Journal of Mining and Geology.* Vol. 56 (2), pp. 319-328.

Ajibade, A.C., Fitches, W.R. and Wright, J.B., 1979. The Zungeru mylonites, Nigeria: recognition of a major tectonic unit. *Revue de Geologie Dynamique et de Geographie Physique*, vol. 21: pp. 359-363. **[Crossref]**

Ajibade, A.C., Woakes, M. and Rahaman, M.A., 1987. Proterozoic crustal development in the Pan-African regime of Nigeria. In: A. KrGner (Editor), Proterozoic Crustal Evolution. *Geodynamic Series, American Geophysics Union,* vol. 17: pp. 259-271.

Ajibade, A.C., Woakes, M. and Rahaman, M.A., 1989. Proterozoic crustal development in the Pan-African regime of Nigeria. In: Kogbe, C.A. (Ed.), *Geology of Nigeria. Elizabethan Publishing Co.*, Lagos, 57-70.

Ajibade, A.C. and Wright, J.B., 1989. The Togo-Benin-Nigeria shield: evidence of crustal aggregation in Pan-African belt. *Tectonophysics*: vol. 165, pp. 125-129 and 433-449. **[Crossref]**

Almeida, F.F.M. and Black, R., 1967. Symposium on continental rift. Montevideo Geological comparison of North-Eastern South America drift and Western Africa. *An. Acad. Brasil. Cienc. (Suppl.)*, pp. 319-377.

Balarabe, B., Lawal, K. M., Ahmed, A. L., Umar, M., Mohammed, M. A. and Adamu, A., 2017. The use of analytic and first derivative techniques to gain insight into aero-magnetic anomaly patterns in part of Ikara, Nigeria. *FUW Trends in Science and Technology Journal*, Vol. 2(2) pp. 684 – 690.

Ball, E., 1980. An example of very consistent brittle deformation over a wide intracontinental area: The Late Pan-African fracture system of the Taureg and Nigerian Shield. *Journal of Tectonophysics*: vol. 16: pp. 363-379. **[Crossref]**

Black, R., Ball, E., Bertrand, J.M.L., Boullier, A.M., Caby, R., Davison, I., Fabre, J., Leblanc, M. and Wright, L.I., 1979. Outline of the Pan-African geology of Adrar des Iforas (rep. of Mall). *Geol. Rundsch.* Vol. 68(2): pp. 543-564. **[Crossref]**

Black, R. and Lie´geois, J.P., 1993. Cratons, mobile belts, alkaline rocks and continental lithospheric mantle: the Pan-African testimony. *Journal of the Geological Society, London,* vol. 150, pp. 89–98. **[Crossref]**

Black, R., Latouche, L., Liegeois, J.P., Caby, R., Bertrand, J.M., 1994. Pan African displaced terranes in the Taureg shield (Central Sahara). *Journal of Geology,* vol. 22: pp. 641-644. **[Crossref]**

Boullier, A.M., 1991. The Pan-African Tran-Saharan belt in the Hoggar shield (Algeria, Mali.Niger): a review. *In:* DALLMEYER, R.D. and LEC'ORC'HE, J.P. (editors) *The West African Orogens and Circum-AtlanticCorrelatives. Springer-Verlag, Berlin*, pp.85-105. **[Crossref]**

Bruguier, O., Dada, S., Lancelot, J.R., 1994. Early Archean component (3.5 Ga) within a 3.05 Ga orthogneiss from northern Nigeria: U–Pb zircon evidence. Earth and Plane tary Science Letters 125, 89–103. **[Crossref]**

Bucher, K., and Frey, M., 2002. Definition, Conditions, and Types of Metamorphism. In: *Petrogenesis of Metamorphic Rocks*. Springer, Berlin, Heidelberg. **[Crossref]**

Burke, K.C. and Dewey, J.F., 1972. Orogeny in Africa; In: African Geology, edited by Dessauvagie, T.F.J. and Whiteman, A.J. *University of Ibadan.* Pp. 583-608.

Burke, K., Dewey, J., and Kidd, W. S. F., 1977. World distribution of sutures – the sites of former oceans. *Tectonophysics*, vol. 40, pp. 66-99. **[Crossref]**

Caby, R., Bertrand, J.M.L. and Black, R., 1981. Pan-African Ocean closure and continental collision in the Hoggar-Iforas segment Central Sahara: *In*

Precambrian Tectonics. Kröner, A. (Editor); Elsevier Amsterdam, pp. 407-434. **[Crossref]**

Caby, R., 1989. Precambrian terranes of Benin- Nigeria and northeast Brazil and the late Proterozoic South Atlantic fit. *Geological Society America Special Paper*, vol. 230, pp. 145-158. **[Crossref]**

Caby, R., Sial, A.N., Arthaud. M., Vauchez, A., 1990. Crustal Evolution and the Brasiliano Orogeny in Northeast Brazil. In: Dallmeyer, R.D.. Lecorche, J.P. (Eds.). West African orogens and Circum-Atlantic Correlatives, Springer-Verlag, pp. 353-376. **[Crossref]**

Dada, S. S., 1998. Crust-forming ages and proterozoic crustal evolution in Nigeria: a reappraisal of current interpretations. *Elsevier Precambrian Research,* vol. 87, pp. 65-74. **[Crossref]**

Dada, S.S., 2006. Proterozoic evolution of the Nigeria-Boborema province; *In: O. Oshin (Editor). The Basement Complex of Nigeria and its Mineral Resources:* A Tribute to Prof. M. A. O. Rahaman*: AkinJinad and Company. Ibadan.* Pp. 29–44.

Dickin, A.P., Halliday, A.N., Bowden, P., 1991. A Pb, Sr, and Nd isotope study of the Basement and Mesozoic ring complexes of the Jos Plateau, Nigeria. Chemical Geology 94, 23–32. **[Crossref]**

Eskola, P., 1963. The Precambrian of Finland, in Rankama, K., ed., *The Precambrian: New York, Interscience Publisher*, pp. 145-264.

Fawwaz, Y. M., 2019. Geology of Mahanga and its Environs, Part of Sheet 103, Ikara SW, Ikara LGA, Kaduna State. *A published M.Sc. Dissertation.*

Ferre, E., Gleizes, G., Bollchez, J.-L. and Nnabo, P.N. 1995. Internal fabric and strike-slip emplacement of the Pan-African granite of Solli Hills. Northern Nigeria. Tectonics, vol. 14, pp. 1205-1219. **[Crossref]**

Ferre, E., De ´le ´ris, J., Bouchez, J.L., Lar, A.U. and Peucat, J.J., 1996. The Pan-African reactivation of contrasted Eburnean and Archaean provinces in Nigeria: structural and isotopic data. *Journal of the Geological Society, London*, vol. 153, pp. 719–728. **[Crossref]**

Ferre, E., Gleizes, G. and Caby, R., 2002. Obliquely convergent tectonics and granite emplacement in the Trans-Saharan belt of Eastern Nigeria: a synthesis. *Elsevier Precambrian Research,* vol. 114, pp. 199–219. **[Crossref]**

Fitches, R.W., Ajibade, A.C., Egbuniwe, I.G., Hole, R.W., Wright, J.B., 1985. Late Proterozoic Schist Belts and Plutonism in Northwestern Nigeria: *Journal of Geological Society London*, vol. 142: pp. 319-337. **[Crossref]**

Garba, I., 2003. Geochemical characteristics of mesothermal gold mineralization in the Pan-African (600 ± 150 Ma) basement of Nigeria. Applied Earth Science: Transaction of the Institute of Mining and Metallurgy, section B, vol. 112(3), pp. 319-325. **[Crossref]**

Garba, I., 2002. Geochemical Characterization of the Gold Mineralization near Tsohon Birnin Gwari, Northwestern Nigeria: *Chemie der Erde/Geochemistry*, vol. 62 (2): pp. 160-170. **[Crossref]**

Grant, N.K., Hickman, M., Burkholder, F.R. and Powell, J.L., 1972. Kibaran metamorphic belt in the Pan-African domain of West Africa. *Nature (London),* vol. 134: pp. 343-349.

Grant, N.K., 1970. Geochronology of Precambrian basement rocks from Ibadan, southwestern Nigeria. *Earth Planetary Science Letters*. Vol. 10: pp. 29-38. **[Crossref]**

Grant, N.K., 1978. Structural distinction between a metasedimentary cover and an underlying basement in the 600 Ma old Pan-African domain of northwestern Nigeria: *Geological Society of America; Bulletin*, vol. 89: pp. 50-58. **[Crossref]**

Hubbard, F.H., 1975. Precambrian crustal development in western Nigeria: indications from the Iwo region. *Geologic Society of America Bulletin*, vol. 86: pp. 548-554. **[Crossref]**

Ibrahim, A.A. and Hayatu, R.A., 2021. Genesis and rare metal potential of pegmatites around Makarfi area, North Western Nigeria. *Journal of African Earth Science.* 178. **[Crossref]**

Leblanc, M., 1981. The Late Proterozoic Ophiolites of BouAzzer (Morocco) evidence for Pan-African plate tectonics: In Precambrian Plate Tectonics. Kroner, A. (Editor): *Elsevier,* Amsterdam. Pp. 435-451. **[Crossref]**

McCurry, P., 1973. The geology of Sheet 21, Zaria, Nigeria: *Overseas Geology and Mining Resources, 45.*

McCurry, P., 1976. The Geology of the Precambrian Palaeozoic rocks of northern Nigeria- review. In: C.A. Kogbe (Editor), Geology of Nigeria. *Elizabethan Publishers and Co., Lagos,* pp. 15-39.

Obaje, N.G., 2009. Geology and mineral resources of Nigeria: *Springer Dordrecht Heidelberg London and New York, pp.* 221. **[Crossref]**

Obiora, S. C., 2006. Petrology and geo-tectonic setting of the Basement Complex rocks around Ogoja, Southeastern Nigeria. *Ghana Journal of Sciences*, vol. 46: pp. 13–46. **[Crossref]**

Odeyemi, I. A., 1981. A review of the orogenic events in the Precambrian Basement of Nigeria, West Africa. *Geologische Rundschau,* vol. 70: pp. 897–909. **[Crossref]**

Oluyide, P.O., 1988. Structural trends in the Nigerian Basement Complex: *Nigerian Mining Geology and Metallurgy Society*, vol. 1, pp. 87-102.

Onyeagocha, A. C. and Ekwueme, B. N., 1990. Temperature-pressure distribution patterns in metamorphosed rocks of the Nigerian Basement Complex - a preliminary analysis. *Journal of African Earth Sciences,* vol. 11, pp. 83-93. **[Crossref]**

Oversby, V.M., 1975. Lead isotope study of aplites from the Precambrian rocks near Ibadan,

Southwestern Nigeria. *Earth Planetary Science Letters*, vol. 27, pp. 177-180. **[Crossref]**

Oyawoye, M.O., 1972. The Basement Complex of Nigeria. In: Dessauvagie, T.F.J. and Whiteman, A J. (Editors), *African Geology,* Ibadan, 1970: *Geology Department, University of Ibadan, Nigeria.* Pp. 67-99.

Rahaman, M. A., 1976. Review of the basement geology of Southwestern Nigeria, in Geology of Nigeria, edited by C.A. Kogbe: *Elizabethan Publishers Company, Lagos,* pp. 41-58.

Rahaman, M. A., 1988. Recent Advances in the Study of the Basement Complex of Nigeria. *Precambrian Research,* vol. 38(1-3), pp. 83-100. **[Crossref]**

Rahaman, M. A., Emofureta, W.O. and Caen Vachetta, M., 1983. The Potassic-granites of the Igbetti area; further evidence of the polycyclic evolution of the Pan-African belt in Southwestern Nigeria. *Precambrian Research.* Vol. 22, pp. 25-92.

Russ, W., 1957. The geology of parts of Niger, Zaria and Sokoto provinces, with special reference to the occurrence of gold: *Bulletin of Geological Survey Nigeria*, page. 27.

Saggerson, E. P. and Turner, L. M., 1972. 24th Institutional Geological Congress, Montreal.

Van Breemen, O., Pidgeon, R.T., Bowden, P., 1977. Age and isotopic studies of some panafrican granites from Northcentral Nigeria. *Precambrian Research,* vol. 4, pp. 307–319. **[Crossref]**

Woakes, M., Rahaman, M. A. and Ajibade, A. C., 1987. Some metallogenic features of the Nigerian Basement. *Journal of African Earth Sciences,* vol. 6(5), pp. 655-664. **[Crossref]**

Wright, J.B., Hastings, D. A, Jones, W.B. and Williams, H. R., 1985. Geology and mineral resources of West Africa. *George Allen and Unwin, London,* vol. 187*,* pp. 111-123.

Yusuf, N. A., Abdullahi, M. and Hassan, I. S., 2018. Geology and Petrography of Basement Rocks around Paki, Northwestern Nigeria. *International Journal of Advances in Scientific Research and Engineering (IJASRE).* Vol. 4 (12). DOI: **[Crossref]**

Yunusa, A., and Ibrahim, A.A., 2023. Structural and lithological controls of pegmatite. Mineralization in Ikara, northwestern Nigeria. *Bima Journal of Science and Technology*, Vol. 7 (1) ISSN: 2536-6041 Pp. 115-122. **[Crossref]**

APPENDIX

MEASURED STRIKE OF THE LINEAMENTS FROM THE LITHOLOGICAL UNITS (ALL MEASUREMENTS ARE IN DEGREES)

1. Migmatitic Gneiss

290	301	135	193	54	275	258	320	358	300	277
300	354	136	193	51	289	188	225	217	263	289
280	310	122	192	14	290	218	268	250	224	136
292	344	123	189	60	300	165	125	165	135	134
290	145	125	191	4	345	78	30	81	135	170
288	154	122	40	210	357	250	54	153	140	120
282	170	135	40	60	278	224	160	122	140	136
311	165	134	10	77	299	263	44	180	135	170
304	114	136	52	88	317	217	280	90	150	135
272	319	130	21	80	319	225	54	180	170	163
315	318	315	53	76	280	188	315	150	134	139
275	313	320	52	32	310	218	340	138	120	155
14	28	20	18	60	310	258	340	135	320	316
20	24	82	179	130	315	275	167	144	315	335

2. Migmatitic (Augen) Gneiss

300	315	354	70	161	4	300	81	21	161
290	279	350	54	162	33	280	83	54	124
299	270	341	32	154	45	289	54	90	134
288	55	333	53	100	89	290	40	150	135
235	66	349	31	171	165	277	39	140	135
279	49	354	69	180	170	300	77	130	140
280	49	311	7	151	315	311	215	161	131
277	230	290	11	161	135	310	210	174	148
315	280	355	53	165	135	350	211	153	
311	310	353	81	149	130	280	210	125	

310	300	271	15	132	132	300	251	121
310	317	359	209	210	131	200	266	170
300	167	290	254	178	137	210	240	176

3. Granite Gneiss

299	304	60	340	296	297	286
354	360	10	335	280	341	352
26	90	70	330	270	285	351
52	12	18	275	292	348	304
30	210	20	55	326	306	273
70	200	33	220	294	300	287
8	208	41	200	290	350	354
12	254	158	189	310	301	280
54	200	110	192	340	280	25
80	200	148	178	324	101	90
14	208	140	124	160	161	12
160	77	155	139	154	94	
100	80	180	111	142	124	

4. Porphyroblastic Gneiss

33	358	310	298	2	110	68
33	349	300	302	22	103	29
145	340	290	243	28	170	324
178	170	313	231	100	170	301
180	175	303	183	194	45	327
358	160	319	190	122	7	301
155	175	304	195	100	9	313
168	177	301	265	152	355	345
169	20	295	9	148	350	251
319	176	181	177	140	163	200
315	119	2	170			
121	160	30	150			

5. Medium-Coarse-Grained Granite

346	263	30	20	300	210	45
365	211	179	51	315	200	28
316	270	160	41	312	250	63
308	211	114	69	312	200	64
357	217	130	35	306	181	20
300	240	110	80	305	201	20
271	215	110	53	208	250	26
280	201	180	71	310	206	203
293	213	215	25	202	189	170
275	245	216	71	204	225	104
300	251	211	62	250	211	180

6. Porphyritic Granite (>Alkali Feldspar)

315	74	128	314	315	334	315
341	32	173	344	199	344	199
280	1	113	323	194	323	194

346	11	180	300	200	300	200
315	70	118	293	190	293	190
279	63	92	312	182	312	182
280	128	318	290	227	290	227
194	146	38	10	108	10	108
223	115	45	49	173	49	173
217	54	70	50	120	50	120
230	129	311	309	135	20	39

7. Porphyritic Granite (>Plagioclase Feldspar)

320	193	104	120	300	60	319
300	99	190	190	303	89	290
290	177	162	155	0	63	
315	11	160	60	300	118	
279	44	180	89	301	102	
348	61	134	63	320	180	
294	1	141	118	299	180	
278	244	160	102	281	117	
304	248	138	180	330	160	
303	300	137	180	319	300	
348	310	152	117	290	301	
284	311	161	160	300	320	
120	289	300	120	289	299	
264	322	303	264	322	281	
264	206	300	264	206	330	

8. Quartzite

173	188	28	132	80	241
34	1	200	210	278	101
346	177	147	184	52	84
167	241	68	190	50	266
178	219	236	128	55	12
32	150	159	142	304	186
198	288	355	20	285	128
130	170	47	176	343	159
17	169	150	70	157	
277	340	69	345	260	
90	224	15	198	251	
225	180	175	84	45	